UNIVERSITY
OF GÄVLE

DEPARTMENT OF TECHNOLOGY

MODEL-BASED PRE-DISTORTION FOR SIGNAL GENERATORS

Carolina Luque

September, 2007

Abstract

Spectrally pure signals are an indispensable requirement when the Signal Generator (SG) is to be used as part of a test bed. However, even sophisticated equipment may not comply with the needs imposed by certain applications. This work approaches the problem by using Digital Pre-Distortion (DPD) based on a polynomial memory-less model obtained for the SG.

Using the SG in arbitrary mode (ARB) an input signal is computer-generated and reproduced by the SG. Measurement accuracy is ensured using coherence sampling and grid matching to the Signal Analyzer (SA). Finally, careful time alignment is used to compare the transmitted and received three-tone signals to obtain the polynomials coefficients.

Results show that the accuracy of the model and the effectiveness of pre-distortion may vary depending on the amplitude of the three-tone signal. However, using polynomials of 5^{th} and 9^{th} degrees up to 15dB reduction of the 3^{rd} order Inter-Modulation products can be obtained, and spurious powers may be lowered down to 70dBc.

Table of Contents

1 Introduction

1.1 Background

When the performance of the high-quality components such as Analog to Digital Converters (ADC) or Power Amplifiers (PA), is measured, special attention should be given to the test setup. The test setup should have much better performance than the DUT which is a demanding requirement. In order to achieve good enough measurements and fulfill the test requirements, while at the same time keeping the cost of the equipment low, techniques for improving the performance of the test setups can be applied.

In some test setups the signal generator (SG) is the weak link. Even state-of-the-art signal generators can have problems to generate spectrally pure signals for some applications. Nonlinearities and other imperfections in the generator result in problems with harmonic distortion and intermodulation products in the generated signal. In this case the SG hardware is insufficient, however spectrally pure signals can be generated by using software techniques.

A modern SG is equipped with an arbitrary waveform generator (AWG), where the waveform is a time series created in a computer program (i.e. Matlab). A method is to generate the wanted signal and measure the actually generated signal. Thereafter calculate the distortion and generate a new signal that is adjusted to compensate for the distortion, a process call predistortion. This is then repeated until the signal purity is sufficient.

1.2 Previous Research

Previous research on pre-distortion was done in [1] describing a method to create pure multi-tone signals using only power measurements. An iterative method for a three-tone signal was developed in [2], however the drawbacks of iterative correction are the large number of time consuming measurements needed and mainly the fact that this method gives a pre-distortion that is unique for a certain signal. An investigation of imperfections in the signal generator was done in [3], where in order to model the signal generator the IQ modulator and the power amplifier were tried separately. A model-based characterization of power amplifiers was developed in [4], considering a memoryless model as well as Hammerstein and extended Hammerstein models (both with memory).

Similar research was performed in [5] and the results agreed with [4] on that the extended Hammerstein system seems to be a useful and accurate model.

Modeling and predistortion design based in Polynomial model for PA was performed in [6]. The simulation results showed that the orthogonal polynomials can alleviate instability problem associated with the conventional polynomials and generally yield better PA modeling accuracy as well as predistortion linearization performance. Another method for pre-distortion based on Look Up Tables (LUT) was applied in [7] for PAs, and the conclusion was that good linearization can be achieved using this technique, and it improves with increasing LUT size. It is also interesting to mention the work done in [8] where predistortions with and without memory are compared for PAs. Memoryless predistortion reduces third order IM (IM3) by 5-8 dB, while memory-based predistortion reduces IM3 by 18-20 dB.

1.3 Problem Statement

To implement Digital Predistortion based on the characterization of a signal generator, in order to obtain spectrally pure signals. Measurement setup considerations, system identification theory, and knowledge about nonlinear behavioural modeling shall be used.

1.3.1 Goals

The main goal is to develop a general automated method using a model-based pre-distortion to generate spectrally pure signals in the range of 60 to 75MHz. The method should be able to manage any kind of signal, without time consuming measurements or exaggerated computational complexity.

1.4 Thesis Outline.

Chapter 1 -Introduction - contains the introduction describing the background, problem statement and the goals to achieve presenting an overview of the contents of this thesis.

Chapter 2 – Theory – presents basic theory about coherent sampling, system modeling, non-linear behavior, and pre-distortion.

Chapter 3 – Test Setup - contains the technical and theoretical information that was used to have the appropriate test setup and measurement procedure along the whole thesis.

Chapter 4 –Methodology - explains the methodology to model the signal generator and design the pre-distorter.

Chapter 5 – Simulation Results - shows the measurements results divided in 3 groups, A, B, and C, for 3 different set of frequencies.

Chapter 6 – Conclusions - presents the conclusions from analysis of the results shown in Chapter 5. Future work is also suggested.

2 Theory

2.1 Introduction

In the present chapter basic theory and definitions are presented. Model-based testing, system identification, nonlinear distortion, behavioral modeling, intermodulation products, signal generator, coherent sampling, and predistortion, will be discussed in order to design a model-based pre-distorter.

2.2 Model-based testing

Model-based testing uses measurements to build a system model that represents certain characteristics of the system's behavior. The system being modeled is commonly referred to as Device Under Test (DUT). Model-based testing has benefits such as the capability of automatically generating many non-repetitive tests or capacity of the test control to automatically run generated tests and is therefore an attractive method to apply.

2.3 Systems and Models

The concept of system can be expressed mathematically by Equation 2.1, where the "black box" N (black box concept is described in section2.3.6) transforms the input $u(t)$ into the output $y(t)$. Figure 2.3 shows a diagram of this relation [9] .

$$y(t) = N(u(t)) \tag{2.1}$$

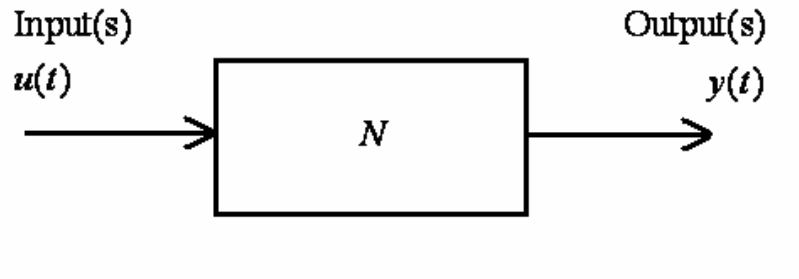

Figure 2.1 "Black box" system, which transforms the input *u*(t) inot the output *y*(t). The matematical expresion of this transformation can be represent by the operator N.

2.3.1 Model Structure and Parameters

The concept of Model is defined as the representation of the real system using a certain set of mathematical functions. The output *M* indicates the mathematical model of physical system, *N*, and can be expressed by [9]:

$$\hat{y}(t) = M(\theta, u(t)) \tag{2.2}$$

Where the symbol "hat", indicates that $\hat{y}(t)$ is the estimated output, *y*(t) of the system. The model *M* will depend on the set of parameters contained in vector θ. To make easier the explanation consider the model $M(\theta)$, as a third-degree polynomial,

$$\hat{y}(\theta, u(t)) = c^{(o)} + c^{(1)}u(t) + c^{(2)}u^2(t) + c^{(3)}u^3(t) \tag{2.3}$$

$$\theta = [c^{(o)}\ c^{(1)}\ c^{(2)}\ c^{(3)}]^T \tag{2.4}$$

The explicit dependence of $\hat{y}(t) = (\theta, t)$ on the parameter vector, θ is shown by Equation (2.3).

Often, models are classified as *parametric* or *non-parametric*. A *parametric* model has relatively few parameters compared to the model coming from direct physical interpretation. In Equation (2.4), each parameter of the vector θ, is related to a particular behavior of the system, that is, the parameter $c^{(2)}$ will define how the output varies with the square of the input.

In contrast, a *non-parametric* model is described by a curve or surface defined by its values at a collection of points in its domain. A non-parametric model usually has a large number of parameters that do not in themselves have any direct physical interpretation [9].

2.3.2 Static and Dynamic System

In general, when a system's current value of the output depends only on the current value of the input, it is call a *static system*. On the other hand, if the system's output depends on some or all the input history, it is said to be a *dynamic system*. Dynamic systems can be further classified according to whether they respond to the past or future values of the input, or both.

2.3.3 Linear and Nonlinear System

In section 2.6 the relation between output and input in a general system was expressed in Equation (2.5). Let *c* be a constant scalar. Then if the response to the input $c \cdot u(t)$ satisfies:

$$N(c \cdot u(t)) = c \cdot y(t) \tag{2.5}$$

For any constant *c*, the system is said to obey the principle of proportionality or to have the scaling property. Equation (2.6) shows two pairs of inputs and their corresponding outputs,

$$\begin{aligned} y_1(t) &= N(u_1(t)) \\ y_2(t) &= N(u_2(t)) \end{aligned} \tag{2.6}$$

If the response to the input $u_1(t) + u_2(t)$ is given by

$$N(u_1(t) + u_2(t)) = y_1(t) + y_2(t) \tag{2.7}$$

Then the operator *N* is said to be obey the superposition property. If the system obeys both superposition and scaling it is said to be a *linear system*.
Nonlinear systems do not obey superposition and scaling. In case that a system obeys the superposition and scaling properties approximately in a restricted range of inputs, the system is said to be operating within its “linear range”.

2.3.4 Time Invariant and Time-Varying Systems

A system is said to be time-invariant when the relationship between the input and output does not depend on the absolute time. A time-invariant system must satisfy [9]:

$$N(u(t)) = y(t) \Rightarrow N(u(t-\tau)) = y(t-\tau), \qquad \forall \tau \in \Re \tag{2.8}$$

The system for which equation (2.8) does not hold is said to be time-varying.

2.3.5 Deterministic and Stochastic Systems

Usually in a deterministic system, the output, $y(t)$, depends exclusively on the input, $u(t)$. However that could be considered as an ideal condition, in practice the output measurement is corrupted by additive noise,

$$z(t) = y(t) + v(t) = N(u(t) + v(t)) \tag{2.9}$$

Equation (2.9) describes a system where $v(t)$ is independent of the input , $u(t)$, and the measured output, $z(t)$, has deterministic and random components. This system is still referred to as deterministic, since the "true" output, $y(t)$, is a deterministic function of input.

When the output depends on an unmeasurable process disturbance, w(t) ,which is the white Gaussian signal, the output cannot be measured.

$$y(t) = N(u(t), w(t)) \tag{2.10}$$

In such case, the system is said to be stochastic, because there is no "noise free" deterministic output. The process noise, in contrast, only appears additively in the final output. Clearly, it is possible for a system to have both a process disturbance and measurement noise that could be expressed using the relation [9]:

$$z(t) = y(t) + v(t) = N(u(t), w(t)) + v(t) \tag{2.11}$$

2.3.6 System Modeling

System modeling determines which terms (described in sections 2.5.2) are significant, and limits the model to relevant terms only. However in this simple case, constructing a mathematical model based only in "first principles" could be impractical. For more complex systems, the approach can become totally unmanageable unless there is good understanding in which effects should not be incorporated into the model. Mathematical modeling problems could be classified according to how much a priori information is available about the system. A white box model is a system where all information is available, and a black box model is a system with no available a priori information [9].

2.3.7 System Identification

A common approach to construct a mathematical model for a given system is system identification; this approach starts from the measurements of the system's behavior and the external influences. A general form, or structure, for the mathematical model is assumed, without going into the details of what is actually happening inside the system, and then the parameters are determined from experimental data [9].

The objective of system identification is to find a suitable model structure, *M*, and corresponding parameter vector, θ, given measurements of the input and output. There are many possible parametric and non-parametric representations or model structures for both linear and non-linear systems. Thus, the physical system, *N*, can be replaced with the model, $M(\hat{\theta})$ and generate:

$$\hat{y}(t) = M(\hat{\theta}, u(t)) \tag{2.12}$$

Where $\hat{y}(t)$ is an estimate of the system output, *y* (t). Similarly, $M(\hat{\theta}, u(t))$ represents the model structure chosen together with a vector of estimated parameters.

Often, instead of having the system output, $y(t)$, only a noise corrupted measurement will be available. Usually, this measurement noise is assumed to be additive, random, and statistically independent of the system's inputs and outputs. The goal, then, is to find the model, $M(\hat{\theta}, u(t))$, whose output, $\hat{y}(t, \hat{\theta})$, "best approximates" the measured output, z(t). The relationship between the system, model, and the various signals, is depicted in Figure 2.4. [9]

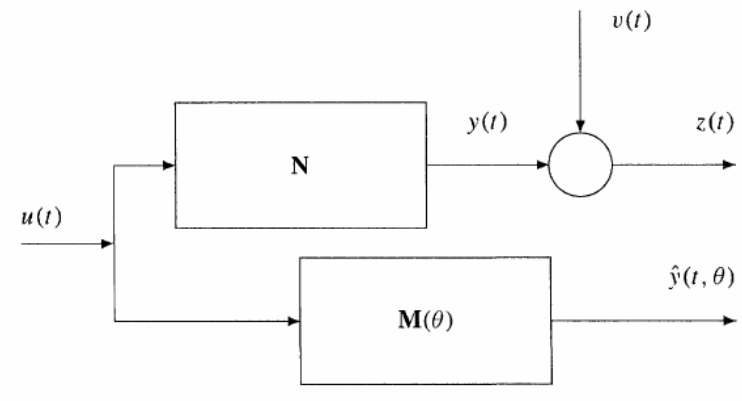

Figure 2.2 The deterministic system identification problem in the presence of the measurement noise

The choice of the identification technique is determined by the details of the model structure. The model can furthermore be identified by minimizing the mean square error of the modeled and measured output signal using the nonlinear least squares estimations methods [9].

Types of System Identification Problems

Many system identification methods are based, either directly or indirectly, on solving an ordinary least-square problem. Such formulations are well suited to dealing with noise in the output signals. However, to deal with noise at the input, it is necessary to adopt a "total least-squares" or "errors in the variables" framework, both of which are much more computationally demanding. To avoid this added complexity, identification experiments are usually designed to minimize the noise in input measurements. In some cases, it may be necessary to adopt a non-causal system description so that the measurement with the least noise may be treated as the input.

The system may also include an unmeasurable process noise input, $w(t)$, and the measured output may also contain additive noise, $v(t)$. Given this framework, there are three broad categories of system identification problem:

- Deterministic System Identification Problem. Find the relationship between $u(t)$ and $y(t)$, assuming that the process noise, $w(t)$, is zero . The measured output, z(t), may contain additive noise, $v(t)$. The identification of deterministic systems usually has the purpose of gaining insight into the system function and this will be the study case along this thesis work.
- Stochastic System Identification Problem. Find the relationship between $w(t)$ and $y(t)$, given only the system output, z(t). Usually, the exogenous input, $u(t)$, is assumed to be zero or constant. This formulation is used where the input is not available to the experimenter, or where it is not evident which signals are inputs and which are outputs.
- Complete System Identification Problem. Given both the input and the output, estimate both the stochastic and deterministic components of the model. This problem formulation is used when accurate output predictions are required [9].

2.4 Signal and Specifications

The present method could be used for any kind of signal, however for this thesis a three tone signal will be used because this signal is suitable to identify the nonlinear terms of the SG.

In general, this signal is defined by:

$$s(t) = r(t)\cos(\omega_c t + \varphi(t)) \tag{2.13}$$

Where ω_c is the carrier frequency and $r(t)$ and $\varphi(t)$ are the envelop and the phase of the signal respectively given by:

$$r(t) = (x^2(t) + y^2(t))^{1/2} \tag{2.14}$$

$$\varphi(t) = \arctan\left(\frac{y(t)}{x(t)}\right) \tag{2.15}$$

Where $x(t)$ and $y(t)$ are the in-phase, I, and quadrature-phase, Q, signals respectively given by:

$$x(t) = \sum_{k=1}^{N} A_k(t)\cos(\omega_k t + \phi_k(t) + \lambda_k) \tag{2.16}$$

$$y(t) = \sum_{k=1}^{N} A_k(t)\sin(\omega_k t + \phi_k(t) + \lambda_k) \tag{2.17}$$

Where $A_k, \phi_k(t), \omega_k$ and λ_k are the amplitude, phase, relative frequency and the initial phase of k:th sub carrier and N is the number of sub-carries. The complex envelope of the input signal in Equation 2.13 is[4]:

$$s_l = r(t)e^{j\varphi(t)} = x(t) + jy(t) \tag{2.18}$$

The frequency range for the three tone signal was selected between 60-75 MHz for purposes of ADC characterization [10, 11].

All the frequencies used in this work were calculated according to coherent sampling theory to eliminate spectral leakage (see section 2.5) as well as taking into account the adjustments needed in order to match the frequency grid between the Spectrum Analyzer (SA) and the Signal Generator to avoid the errors in the measurement process.

2.5 Coherent sampling

Coherent sampling is a technique to evaluate the dynamic performance of fast and ultra fast data converters. In this method when certain conditions are met, the spectral resolution of an FFT is increasing and the need of window sampling is eliminated.
Mathematically it can be expressed as :

$$f_{in} / f_{sample} = N_{window} / N_{record} \tag{2.19}$$

f_{in} : Periodic input signal

f_{sample} : Sampling clock frequency of the ADC under test

N_{window} : Integer number of cycles within the sampling window

N_{record} : Number of data points in the sampling window or FFT.

f_{sample} / N_{record} : Size of one frequency bin.

The main purpose of applying this technique is to reduce the spectral leakage. Thereby, the main key in this technique is to force an integer number of input cycles within the sampling window to select the sinusoidal input test tones, Figure 2.1.

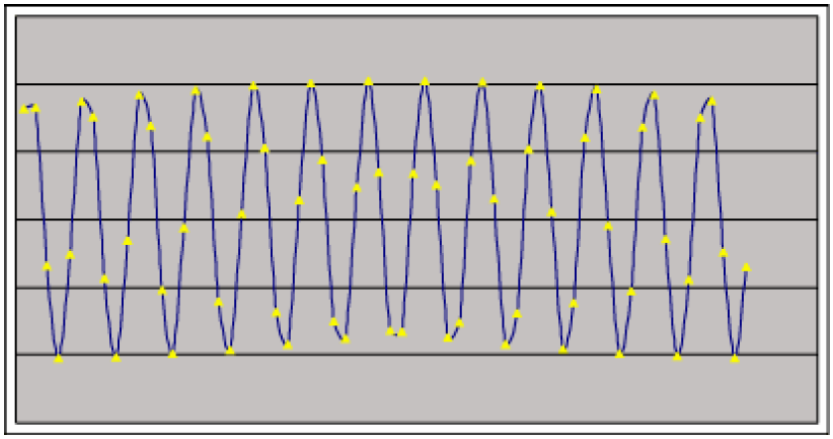

Figure 2.3: Coherent Sampling .

The wave form is considered continuously sampled from minus infinity to plus infinity in its FFT. As it was mentioned, if the above condition expressed by equation (2.1) is not met, spectral leakage occurs.

Spectral leakage distorts the digitized result by spreading the energy of any given frequency component across adjacent frequency bins. There are two ways to reduce the spectral leakage, coherent sampling and window sampling. Nevertheless, coherent sampling produces the best quality in high resolution FFTs [12] in evaluation of dynamic performance of ADCs. Therefore all the frequencies used in this work will be set according to coherent sampling.

2.6 Spectral purity

Nonlinear and non-ideal components in signals sources, introduce components that are needed to provide a broad range of frequencies and output power, however they also introduce phase noise and unwanted distortion products.

All these impairments produce spurious over the wanted signal, then, spectral purity is defined as the difference between the smallest wanted component and the highest unwanted component, and mathematically could be expressed as [2]:

$$\text{Spectral purity [dBc]} = P_{\text{smallest wanted component}}\ [\text{dBm}] - P_{\text{biggest wanted component}}\ [\text{dBm}] \quad (2.20)$$

2.7 Intermodulation (IMD)

Intermodulation (IMD) is the formation of combination frequencies resulting from a nonlinear transfer characteristic when several frequencies components from the input signal. The third order intermodulation products usually gives the most of the problems, since their frequencies are close to the fundamental frequencies.

2.8 Pre-Distortion

Pre-distortion (PD) is a technique consisting basically of introducing the inverse of the unwanted characteristic of the DUT, K^{-1}, in series with the DUT, to eliminate the distortion introduced by the unwanted DUT's characteristic. A block diagram of this concept is shown in Figure 2.4.

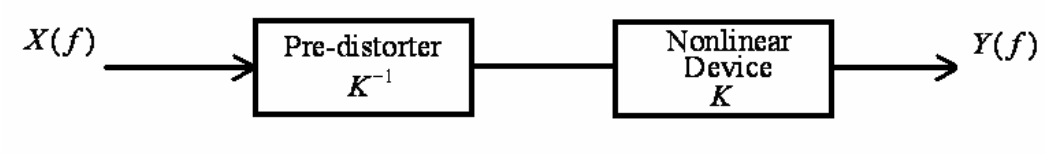

Figure 2.4: Pre-distortion main idea

Pre-distortion can be realized in two ways:

- Digital implementation
- Analog implementation.

Digital Pre-Distortion (DPD) is simpler compared to feedforward linearization widely used in base stations [13]. Since the implementation of DPD, is done with digital components, the system is more robust and flexible than analog circuits. However, all data samples must be modified continuously, and high amount of mathematical operations in digital domain is required. If sampling frequency or bandwidth of the modulation signal increases, then the required clock frequency and amount of operation also increase. High clock frequency or high amount operations mean higher power consumption, thereby; a drawback of DPD is its limitation in bandwidth. Fortunately the continuous improvement in digital IC technology makes DPD a promising linearization technique for future applications.

If the system is not frequency dependent, then it can be assumed that the output depends solely on the momentary input signal, and this case is noted as the static case.

In static case, also known as memoryless case, the applications are mainly of two different DPD types:

- Look up table (LUT) based pre-distorter [7] and
- Polynomial pre-distorter [6].

LUT based pre-distorter stores the pre-distortion coefficients for all input values in the LUT and the incoming signal is multiplied sample by sample with this coefficient.

In the polynomial pre-distorter case, the characteristics of the SG and the pre-distorter are described by polynomial functions. The polynomial coefficients of the pre-distorter are adjusted to compensate the DUT nonlinearity, resulting in a linear system. In this thesis, a polynomial pre-distorter will be studied; it was selected based on the following reasons:

- Even though the adaptation algorithms for a polynomial pre-distorter are computationally more intensive compared to algorithms for the LUT-based pre-distorter, the analog circuit in polynomial pre-distorter case, is easier to implement.
- Digital pre-distortion is a useful method to achieve linearity improvement in mobile transmitters, where the simplicity and almost zero cost of a simple pre-distorter is well worth the few decibels of ACP or IM reduction that can be obtained over a limited power range [14].

2.9 Memoryless system (The Static Model)

A simple approach to model the signal generator is to use a memoryless polynomial model where the output could be estimated using the following equations:

$$y(t) = N(u(t))$$

$$\hat{y}(t) = M(\theta, u(t)) \tag{2.21}$$

$$\hat{y}(n) = \sum_{i=1} \theta_i u^i(n) \tag{2.22}$$

The block diagram of the static model is show in Figure 2.1.

Equation 2.15 represents the signal generator's system and the task now is to find the values of θ_i coefficients. There is more than one solution for this system, and in order to find the best possible set of parameters θ_i, that makes the estimated output as close as possible to the real output, a least square estimation method [15] could be used. The method consists of minimizing the squared error given by:

$$\frac{\partial \varepsilon}{\partial \theta_i} = 0; \forall i \tag{2.23}$$

where:

$$\varepsilon = \sum_{n=0}^{\inf} \left| e(n) \right|^2 \tag{2.24}$$

$$e(n) = y(n) - \hat{y}(n) \tag{2.25}$$

$y(n)$: Measured output .

$\hat{y}(n)$: Estimation output.

$e(n)$: Estimation error (error between the $y(n)$ and $\hat{y}$ (n))

However in practice, the error of the model will never be zero. Therefore, the performance of the model is determined by how much the mean squared error can be minimized.

2.10 Model with Memory

A model is said to have memory when the output of the Signal Generator is not only a function of the current input, with some constant delay, but it also depends of the previous input values [16].

2.10.1 Hammerstein Model

The Hammerstein model consists of a nonlinearity $N(\cdot)$ followed by a linear filter $H(\cdot)$ as shown in the Figure (2.5) [16]:

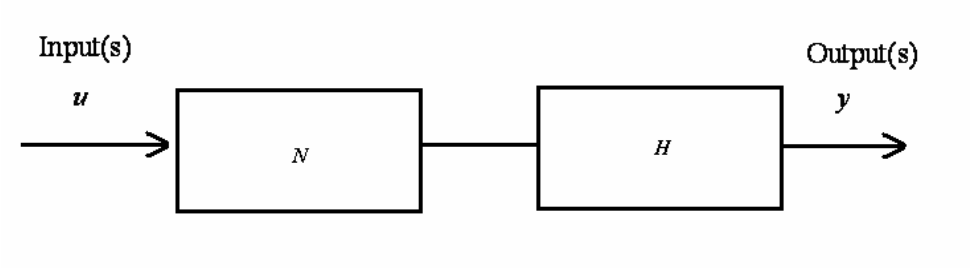

Figure 2.5 Block structure of the Hamerstein model

The output of this model can be written as:

$$y(n) = N(u(n))H(q) = \sum_{m=0}^{M} b_m \sum_{p=1}^{P} h_{2p-1} \left|u(n-m)\right|^{2(p-1)} u(n-m) \qquad (2.26)$$

where:

M : Number of previous samples considered, i.e. the memory length of the model.

N : Polynomial of P coefficients of order 2P-1,

b_i : Coefficient of N(·)

h_i : Coefficient of H(·)

The Hammerstein model is not further studied in this thesis, but it would be an interesting future work.

3 Test Setup

3.1 Introduction

This chapter presents an overview of the implemented test system, internal structure and configuration of the instruments used, measurement techniques, and some important considerations made during the measurements, in order to improve the perfomance of the setup system. The test setup consists of a Rhode & Schwarz SMU200A Vector Signal Generator (SG) , a Rhode & Schwarz FSQ 26 Signal Anayzer (SA), and a personal computer (PC) interconected to arrange an appropriate measurement enviroment for the DUT characterization, see Figure 3.1.

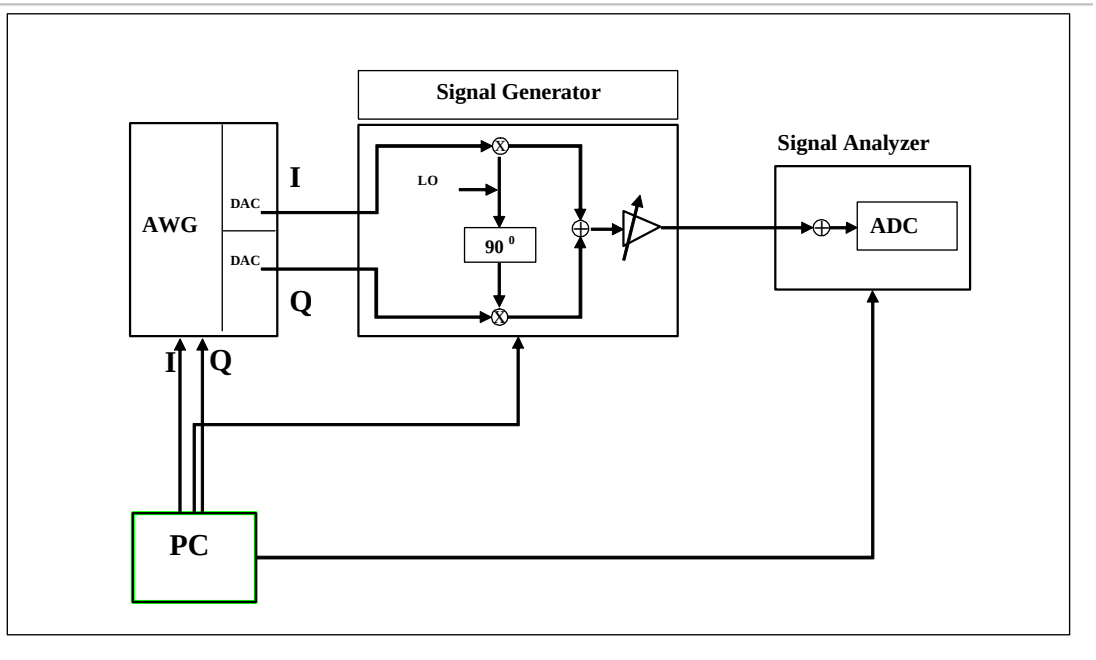

Figure 3.1. The measurement system used for the measurements presented in this thesis.

3.2 The implemented System

Figure 3.1 shows the system setup used, details are given in [4]. The instruments mentioned in section 3.1 were interconected as follows:

- The PC was connected to the SA via a 100 Mbits/s Local Area Network (LAN).

- A GPIB card allowed the connection between the SG and PC.
- SG and SA are equipped with network interface. An RSIB interface, Matlab software and functions from the instrument control toolbox were used for the remote control interface.

A signal according to coherent sampling is generaterated in the PC, as I (In-phase) and Q (Quadrature phase) values, and down loaded to the Arbitrary Waveform Generator (AWG). The AWG generates the analogue I and Q signals at baseband and these signals are introduced to the I-Q modulator of the signal generator. An RF output signal is obtained as given by (3.1) and its complex envelope is defined by (3.2).

$$\begin{aligned} s(t) &= r(t)\cos(\omega_c t + \varphi(t)) \\ s(t) &= x(t)\cos(\omega_c t) - y(t)\sin(\omega_c t) \end{aligned} \tag{3.1}$$

$$s_l(t) = x(t) + jy(t) \tag{3.2}$$

where :

$s(t), s_l(t)$: Are the general signal and the bandpass representation[4].

$r(t), \varphi(t)$ ω_c : Are the envelop, phase and carrier frequency respectely.

$x(t), y(t)$: Are the in-phase and quadrature phase respectely.

According to Section 2.3, the obtained output can be represented by equation 2.1, where ***N*** is a general nonlinear system that will represent the DUT, $u(t)$ and $y(t)$ are the input signal and output signals. The output signal is read from the SA, down converted and digitalized by the signal analyzer and sent back to the PC, as I and Q values, to be analyzed. The analysis is done in order to perform the characterization of the SG. Then using this information to helps generating the new pre-distorted signal, which will be introduced again into the SG .

3.3 Vector Signal Generator

The R&S SMU200A vector signal generator used in this measurements, has two independent signal generators in one cabinet with two analog to digital converters up to 100MHz, and it is equipped with and arbitrary wave generator (AWG). The frequency

range is required between 60 to 75 MHZ. From Nyqvit's sampling theorem the sampling frequency (SF) must be twice the desired frequency. However the SMU200A SG has a limited SF of 100MHz. Hence, in order to reproduce the desired signal, a new set of frequencies relative to the carrier frequency were introduced in the AWG and modulated by the SG. This procedure was followed to generate the desired signal despite the frequency limitations of the instruments.

The SG used offers several types of modulation, but it was set to the ARB mode. ARB mode does a playback from internal memory of the In-phase and Quadrature components of the MATLAB generated signal. In this mode any signal will be resampled to 100MHz and then output, which limits the bandwidth to 0.31 of the sampling rate. Figure 3.2 illlustrates the procedure.

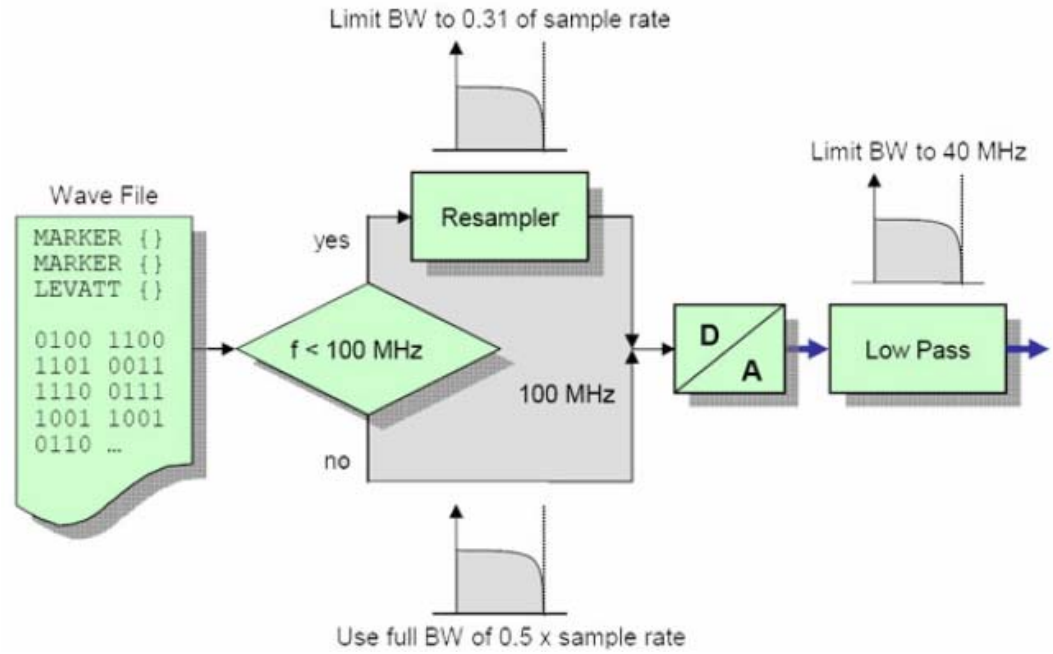

Figure 3.2 Block diagram of the ARB generator.

3.4 Measurements techniques

3.4.1 Equalization

To achieve accurate characterization for the signal generator there are certain considerations. One must make sure that there is a match between the SG and SA grids, so that each frequency from the SG falls in only one bin in the SA. The bin width of the SA is given by:

$$Bin\_width = \frac{f_s}{M} \tag{3.3}$$

Where:

f_s : Is the sampling frequency.

M : Is the number of samples points.

The number of sweep points, represented by *n_sweep* is equal to 5001, then, the frequency span could be calculated as follows:

$$Span = n\_sweep \times Bin\_width \tag{3.4}$$

$$span = f_{stop} - f_{start} \tag{3.5}$$

Where f_{stop} and f_{start} are stop and start frequencies respectively. To match the SG and SA grids the start and stop frequencies are recalculated:

$$f_{new\_stat} = f_{start} - \left(\frac{Bin\_width - 1}{2} \right) \tag{3.6}$$

$$f_{new\_stop} = f_{start} + Span - \left(\frac{Bin\_width - 1}{2} \right) \tag{3.7}$$

3.4.2 Signal Analyzer.

FSQ's internal architecture, is capable of measuring an outputting the magnitude and phase of the signal in addition to its power values. Figure 3.3, shows the analyzer hardware from the IF to the processor.

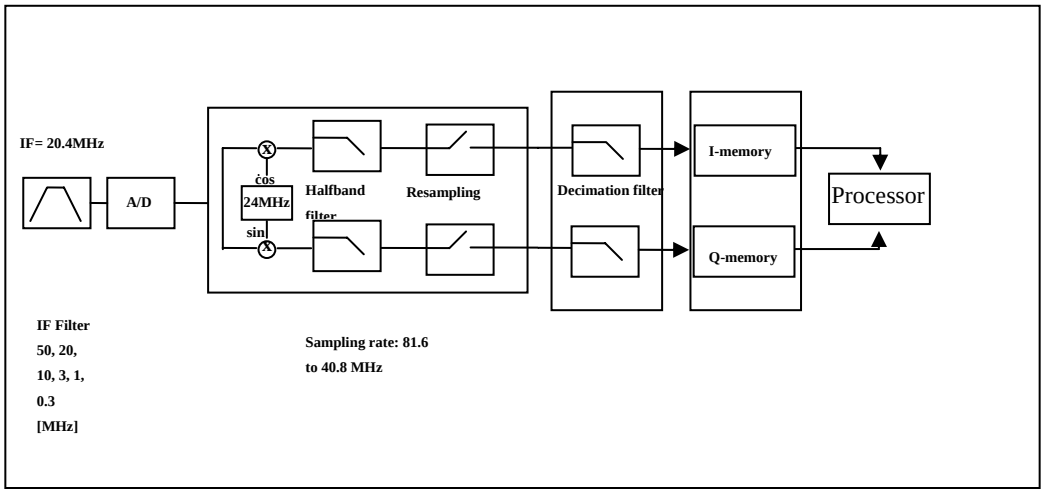

Figure 3.3 Analyzer hardware from the IF to the processor. The IF filter is the resolution filter of the spectrum analyzer and can be set between 300 kHz and 50 MHz.

In the present SA a down conversion to the complex baseband is done after the lowpass filtering and reduction of the sampling rate, the output sampling rate could be set between 10KHz to 81.6 MHz.

There is a complication regarding the SA that limits the ability to analyse small resolution bandwidths due to the fundamental property of the FFT algorithm itself. Considering that FFT is a baseband transform, this means that the FFT frequency range, starts from 0 Hz, (DC voltage) and extends to the maximum frequency (half of the sampling frequency f_s). If small frequency bands need to be analyzed, it will represent a serious problem. Though control of the frequency span by varying the sampling rate is possible, the resolution is still limited because the start frequency of the span is DC.

The *zoom operation* or *zoom mode*, is a solution to the previously mentioned limitation, since it allows a redution of the frequency span while keeping constant the center frequency. It is useful because it facilites analyzing and viewing small frequency components away from 0 Hz. The *zoom* operation is a process of digital quadrature mixing, digital filtering, and decimating/resampling as illustrated in Figure 3.3. The frequency span of interest is mixed with a complex sinusoid at the zoom span center frequency (f_z), which causes the frequency span to be mixed down to baseband. Thus, the signals are filtered and resampled for the specified span, and all out-of-band frequencies are removed [17].

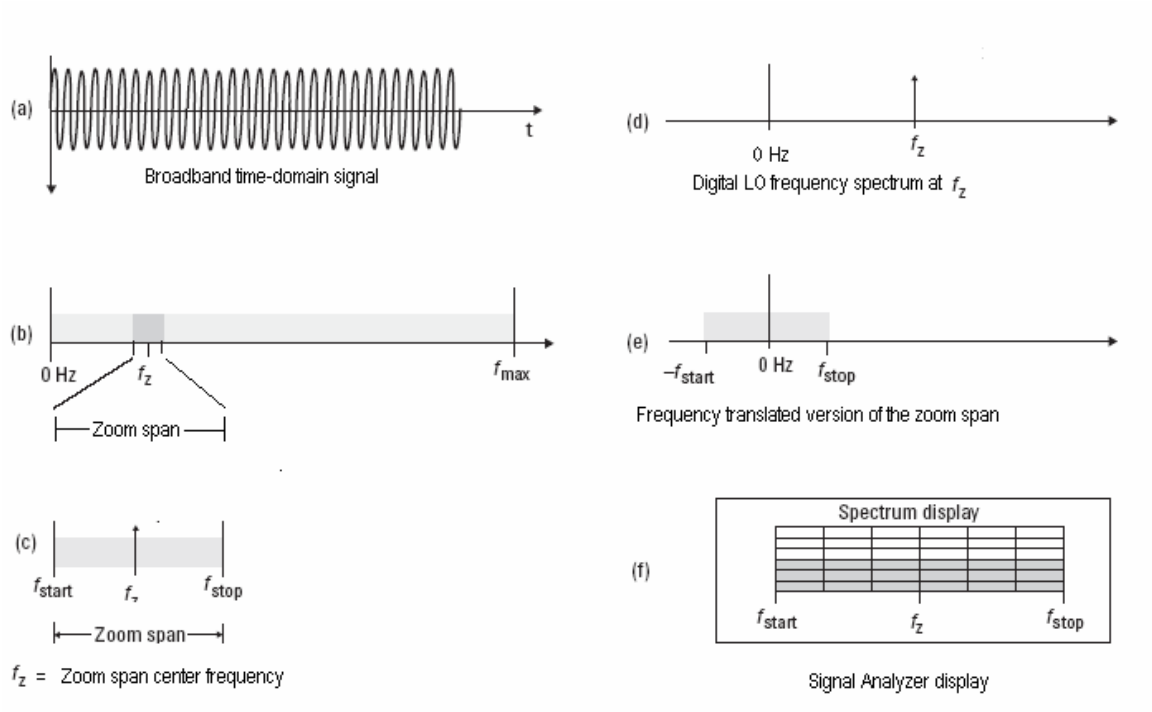

Figure 3-4 Band selected analysis (zoom mode): a) measured broadband signal, b) spectrum of the measured signal, c) selected zoom span and center frequency, d) digital LO spectrum (at zoom center frequency), e) frequency span mixed down to baseband, f) display spectrum annotation is adjusted to show the correct span and center frequency.

This chapter gave a brief overview of the implemented system setup, procedures and used equipment for performing characterization of the DUT. Several important things were established. First of all, the good sincronization between the SG and the SA is crucial for getting realiable values in order to perform accurate and robust charaterization of SG. This determines the quality of the model-base pre-distorter.

4 Methodology

4.1 Introduction

In this section the methodology to characterize the signal generator to develop the model-based pre-distortion will be described. The first step was to obtain the behavioral characteristics of the signal generator to find its model. Since the SG was assumed a memoryless system a single polynomial model was required to model the SG. System identification theory and an appropriate test setup were a requirement to obtain an accurate model of the SG. The second step was to use the coefficients of the polynomial model found for the signal generator to desing the model-based pre-distorter.

4.2 Characterization of the Signal Generator

To characterize the signal generator a three tone signal was used, see section 2.4. The signal was introduced in complex base band notation, and only the odd order terms were considered, since those terms give an output signal in the fundamental zone around the carrier frequency *fc* [16]. To keep the phase angles to ensure that the I and Q components of the signal are not shifted, the complex part of these values were conserved. Also, the system was assumed to be memoryless, i.e. a static model behavior. Then, considering the two aspects mentioned above (system without memory effects with only odd order and complex values) the input signal can be expressed as [2]:

$$u^{2k+1} = \left|u^{2i}\right| \cdot u \tag{4.1}$$

Then, equation (2.3) can be rewritten as follows:

$$\hat{y} = \theta_1 u + \sum_{i=1} \theta_{2i+1} \left|u\right|^{2i} \cdot u \tag{4.2}$$

A memoryless polynomial of the 7^{th} and 9^{th} degree were developed, however the mathematical analysis for the 7^{th} degree will be presented. Thus equation (4.2) becomes:

$$\hat{y} = \theta_1 u + \theta_3 u^2 \cdot u + \theta_5 u^4 \cdot u + \theta_7 u^6 \cdot u \tag{4.3}$$

To simplify the software implementation, matrix notation was used [16]:

$$H = \begin{bmatrix} u \\ u.|u|^2 \\ u.|u|^4 \\ u.|u|^6 \end{bmatrix} \tag{4.4}$$

The nonlinear model behaviour is represented by *H*. An optimal model predictor can be expressed as:

$$\theta = \begin{bmatrix} \theta_1 & \theta_2 & ... & \theta_i \end{bmatrix}^T, \theta: \text{ parameter vector} \tag{4.5}$$

$$\hat{y} = \theta * H \tag{4.6}$$

Hence

$$\hat{y} = \left[\theta_1 u(n) + \theta_2 |u(n)|^2 u(n) + \theta_3 |u(n)|^4 u(n) \right] \tag{4.7}$$

A good solution of equation (4.6) that minimizes the mean square error can be expressed in matrix form as [16]:

$$H'.H.\theta = H'.y(n) \tag{4.8}$$

where:

H : Is a matrix having each power order of the input in a separate column.

H' : Is a transpose of H

θ : Is a column vector of the measured output values.

To find the θ_i coefficients, equation 4.5 can be rearranged into:

$$\theta = inv(H'.H).H'.\hat{y}(n) \tag{4.9}$$

4.3 Pre-distortion

The design Methodology developed in this Chapter is based mainly on the non-linear modeling methods discussed in Chapter 2. A few observations which should be remembered through all that follows in the Chapter are [14]:

1. The process clearly runs into difficulties: There is a point of not return, where no further increase of drive level can move the output to the desired point on the linear characteristics. This issue assumes significance in communications systems, where signals having high Peak Envelope Power (PEP) to average power ratio are commonly used.
2. The signal emerging from the pre-distorter will be highly distorted. This observation can have a critical impact in terms of the required bandwidth of the PD and\or the speed of the DSP circuitry; it may also have more far-reaching implications as high-speed data signals spread to fill up the entire bandwidth of interest.

This work presents results for a pre-distortion based in polynomials of fifth and ninth degrees, those polynomials were built using the coefficients of the modeled SG with inverted sign. The new additional higher order term distortion introduced by the pre-distorter, which were absent in the original SG were assumed neglecting small.

As was mention in section 4.2, there is not need to compensate some terms to considering their contribution to the disturbing distortion neglecting small. However, in order to more effectively cancel these terms a pre-distorter of higher order may be needed. A second measurement could also be taken and parameters obtained could be added to the first set of parameters to improve the results.

5 Simulation and Results

5.1 Introduction

This chapter presents measurement results from model-based pre-distortion applied to the Signal Generator. The input signal used to develop the pre-distorter was a three tone signal with a frequency range between 60 – 75 MHz [11], with equal amplitude and equal phase shift, for each of the tones.

The pre-distortion developed was digital pre-distortion (DPD) for the memoryless polynomial case, it was based on the behavior characteristics of the SG. The methodology was explained in Chapter 4.

The test setup used along all measurements was described in Chapter 3. The model characterization of the signal generator was performed with a frequency span of 50 MHz; however the figures corresponding to the measurements will zoom the most interesting 30 MHz. The resolution bandwidth (RBW) was set to 2 kHz in order to achieve high enough signal-to-noise ratio (SNR) without falling into long sweep times, and it was selected from the direct observation of the performance of the spectrum analyzer. It is relevant to mention that the effect from the carrier frequency, established at 60 MHz, can be reduced by tuning the I and Q-offset. However, this is not covered by this thesis.

5.2 Measurements

The measurement results may be divided in 3 groups: A, B and C. Groups A and B used a three tone test signal at 3 different sets of frequencies:

- Case I : frequencies at 65, 69, 71 MHz,
- Case II: frequencies at 67, 70, 71 MHz and
- Case III: frequencies at 67, 68, 71 MHz.

In Group C two different average input power levels for only one set frequencies (case III) was used.

Group A (general model)

Measurements of Case I of Group A were used to find the general model coefficients for the SG. This set of coefficients was used to develop digital pre-distortion (DPD) of fifth and ninth polynomial degree, and the same digital pre-distorter was applied to correct the three sets of frequencies (case I, II, and II).

The three tones in each set frequencies had amplitude set to -10 dBm and phase of 0^o degrees (see section 2.4). The results obtained for group A are summarized in tables 5.1, 5.2, and 5.3.

Group B (individual model)

In group B, for each set of frequencies different SG model coefficients were calculated. The pre-distorter built upon those coefficients was used to correct its corresponding case. That means that three models for the SG and three pre-distorters were designed. The amplitude for the three cases of frequencies was equal to -5 dBm and phase shift of $0\ ^o$. For details on this group results refer to tables 5.4, 5.5, and 5.6.

Group C (amplitude dependence)

Group C required two different input power levels (-5 and -10dBm, and one set of frequencies (case III) to design the pre-distorter. The polynomial order used for this pre-distorter was of ninth degree. The phase in between the three tones was of 0^o degrees. Detailed information is shown in in tables 5.7, 5.8, and 5.9.

Groups A and B have plots showing measurement results of the power spectrum of the SG, without pre-distortion and with pre-distortions of fifth and ninth degrees. Group C illustrates the power spectrum of the SG without pre-distortion and with pre-distortion of ninth degree.

The main purpose of groups A and B and was to check the reliability of the model obtained for the SG. Group C was used to study the possible differences in the pre-distorted responses and their amplitude dependence.

The analysis of measurement results will focus on the spectral purity achieved with the DPD and the polynomial degree required to reach that spectral purity. The reliability of the SG model will also be discussed, and close attention will be paid to the highest amount of reduction of spurious levels, and where does it come from (IMD products, harmonics, or another nonlinear source).

Group A

The model coefficients, used to design the pre-distorter, were computed from the case I, and applied to case I, II, and III. As was mentioned, the amplitude between the tones is the same and it is equal to -10 dBm, the phase shift was also the same for all tones and equal to 0^o degrees.

Case I

Figure 5.1 shows the power spectrum of the SG without pre-distortion for case I. Figures 5.2 and Figure 5.3 exhibit the power spectrum with pre-distortion of fifth and ninth polynomial degree respectively.

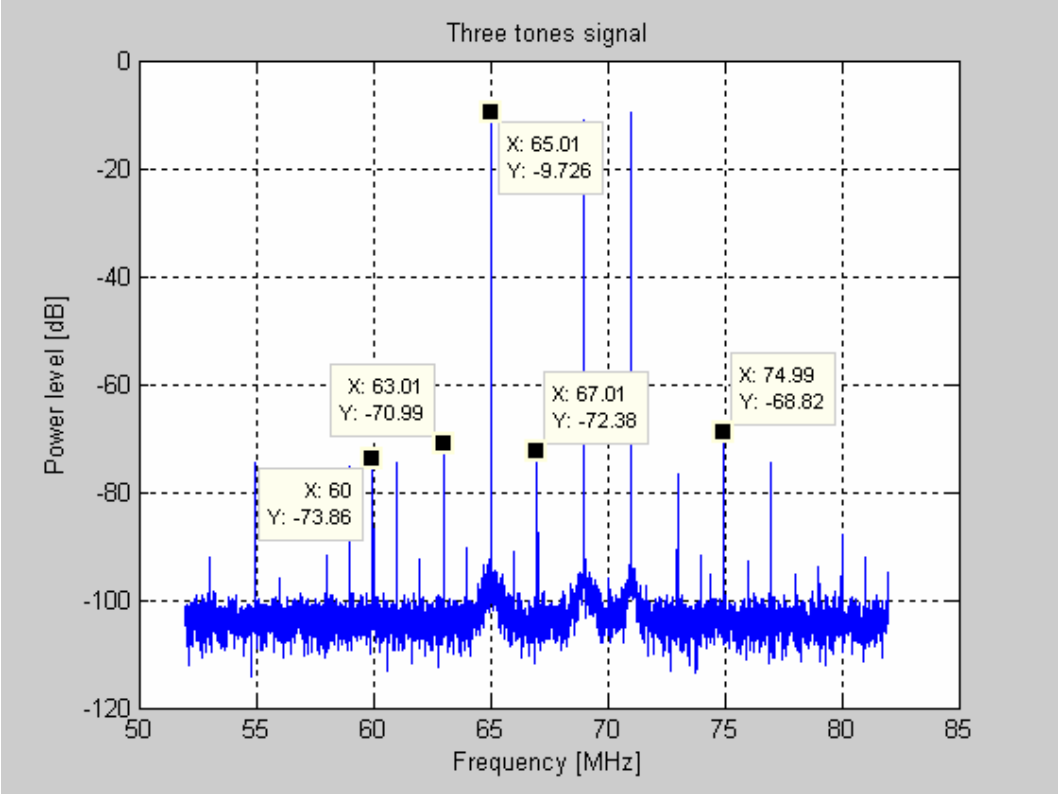

Figure5.1 Power spectrum of the SG without pre-distortion, case I

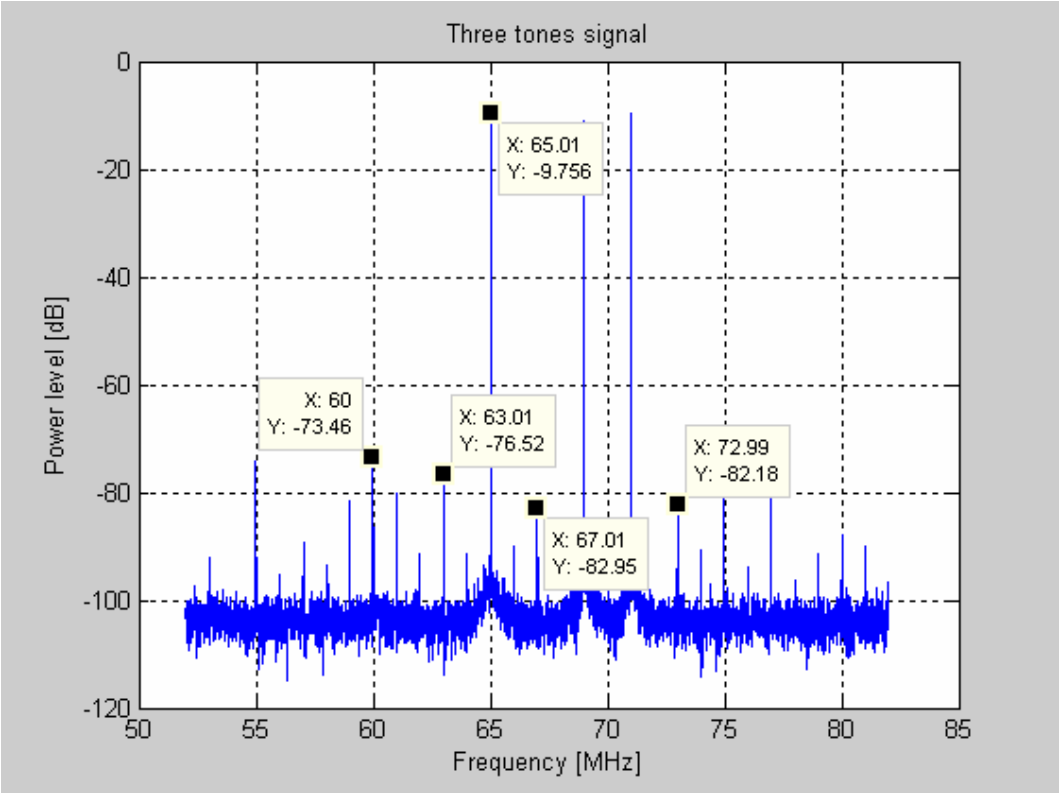

Figure 5.2 Power spectrum of the SG with pre-distortion of the fifth polynomial degree , Case I

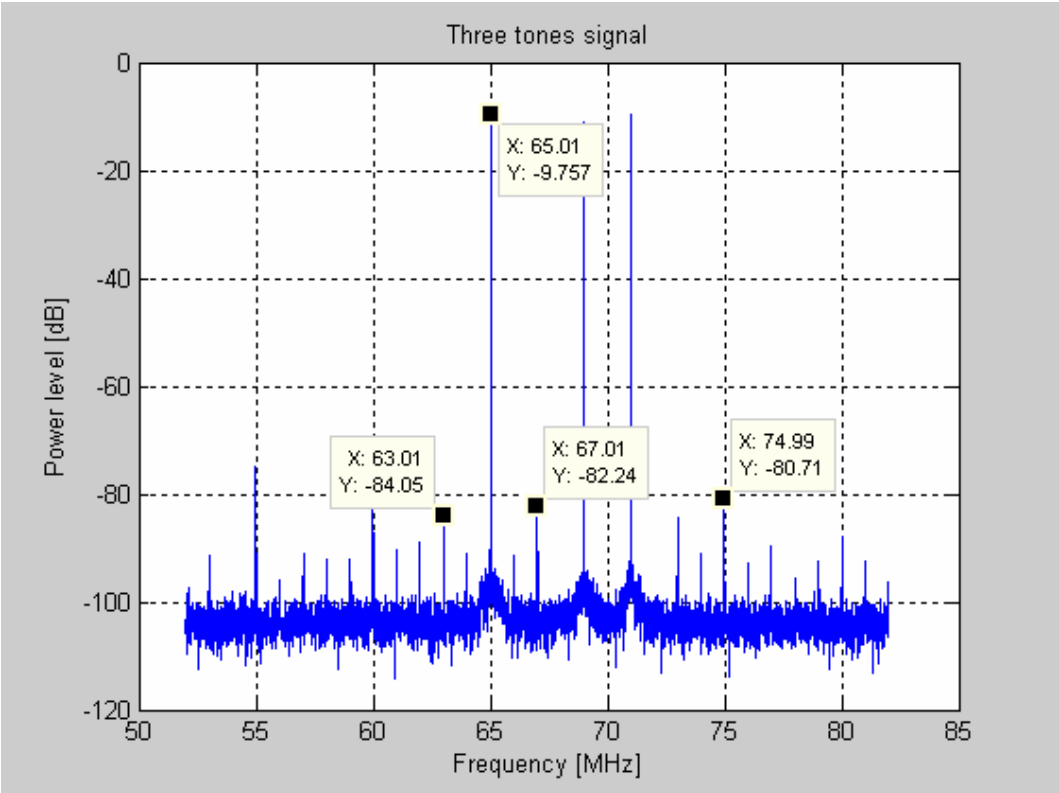

Figure 5.3 Power spectrum of the SG with pre-distortion of ninth polynomial degree, Case I.

The results shown in figures 5.1, 5.2 and 5.3 are summarized in table 5-1, which contains information about the power levels for the wanted and IMD frequencies before and after correction with pre-distorters of fifth and ninth polynomial degree. It also shows the improvements and the final spectral purity achieved.

IMD & Three tone frequencies	Frequency [MHz]	Power Level (PL), without predistortion [dBm]	PL with predistortion of fifth degree [dBm]	PL with predistortion of ninth degree [dBm]	IM5 Reduction Spurious levels [dB]	IM9 Reduction Spurious levels [dB]
-	54.98	-74.66	-74.22	-74.86	-0.44	0.2
2*f1-f3	59.03	-75.43	-81.7	-92.11	6.27	16.68
fc	60.00	-73.86	-73.86	-74.61	0	0.75
f1+f2-f3, 4*f2-3*f3, 4*f2-3*f3	63.01	-70.99	-76.52	-84.05	5.53	13.06
f1	**65.01**	**-9.726**	**-9.726**	**-9.757**	**0**	**0.031**
2*f2-f3, f1-f2+f3	67.01	-72.38	-82.95	-82.24	10.57	9.86
f2	**69.00**	**-10.93**	**-10.97**	**-10.93**	**0. 04**	**0**
f3	**71.00**	**-9.627**	**-9.632**	**-9.636**	**0.005**	**0.009**
2*f2-f1, 2*f3-f2	72.99	-76.7	-82.18	-84.42	5.48	7.72
2*f2-f1, 3*f3-2*f2	74.99	-68.82	-74.09	-80.71	5.27	11.89
2*f3-f1 , 4*f3-3*f2 , 4*f3-3*f2 , 3*f2-2*f1	76.99	-74.49	-79.57	-89.55	5.08	15.06
Spectral Purity [dBc]		57.9	63.12	69.12	5.22	11.22

Table 5-1 Summary of the results using a general model in the pre-distortion for SG, case I

From table 5-1 one can see that the highest spectral purity is achieved for pre-distortion of ninth degree, and is equal to 69.12 dBc. The greatest reduction of spurious levels was of 16.68 dBm for an IM3 frequency.

Case II

Measurements with tones at 67, 70, and 71 MHz gave the results presented in the following figures:

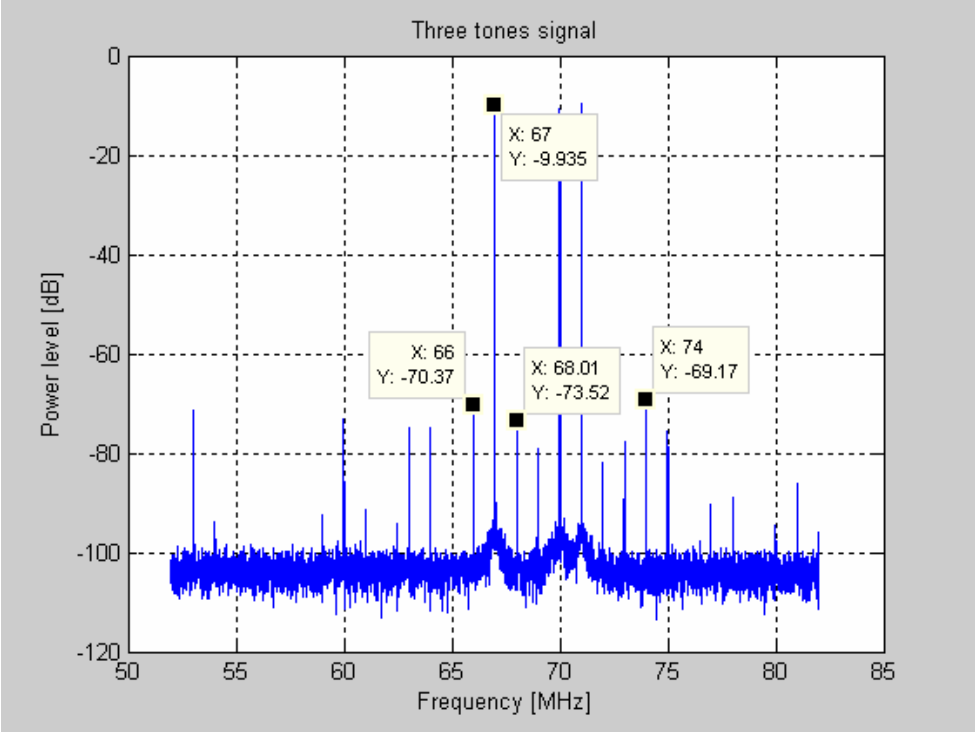

Figure 5.4 Power spectrum of the SG without pre-distortion, Case II

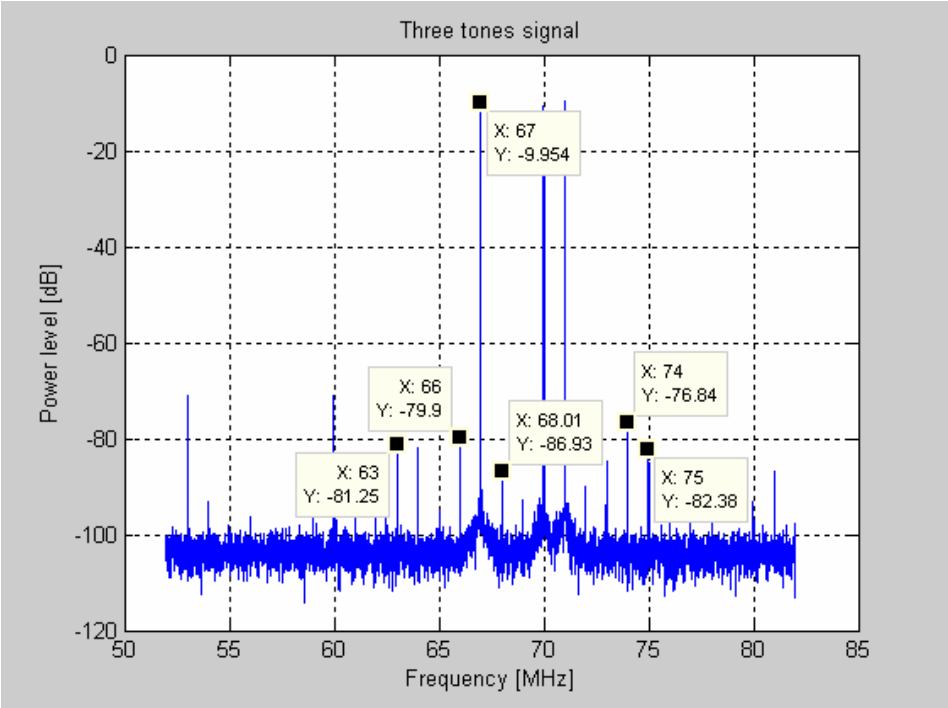

Figure 5.5 Power spectrum of the SG with pre-distortion of the fifth polynomial degree, Case II

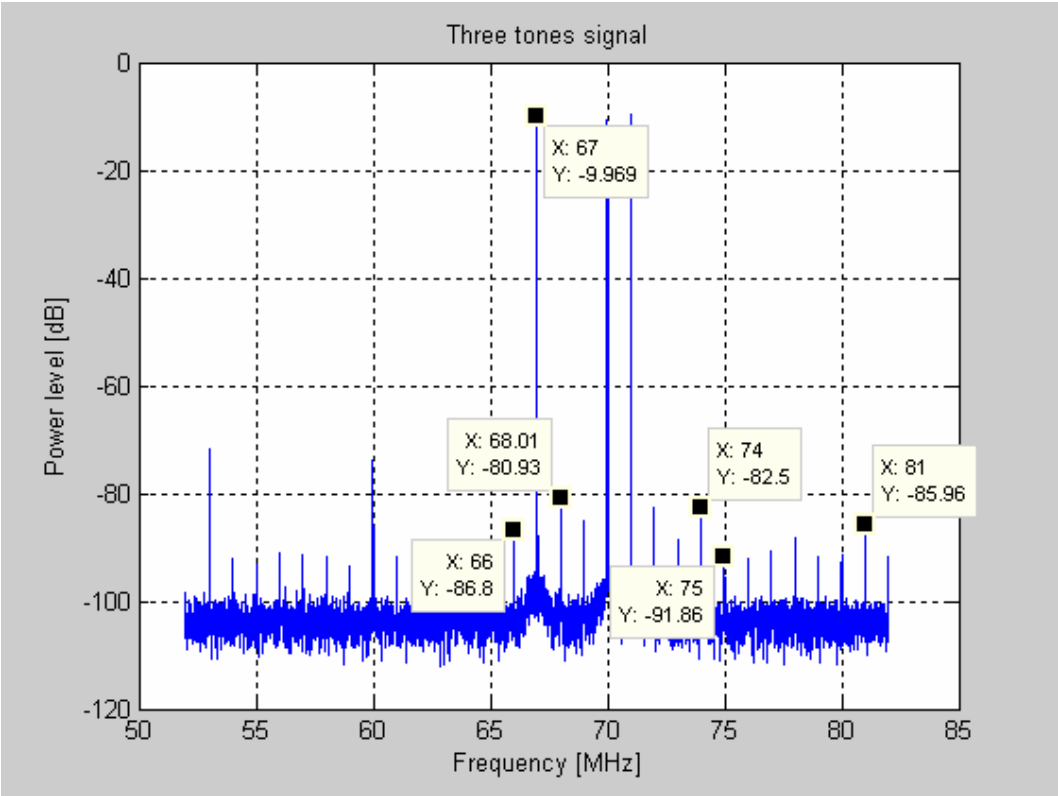

Figure 5.6 Power spectrum of the SG with pre-distortion of the ninth polynomial degree, Case II

IMD & Three tone frequencies	Frequency [MHz]	Power Level (PL), without predistortion [dBm]	PL with predistortion of fifth degree [dBm]	PL with predistortion of ninth degree [dBm]	IM5 Reduction Spurious levels [dB]	IM9 Reduction Spurious levels [dB]
-	53	-71.43	-71.11	-71.65	-0.32	0.22
fc	60	-73.06	-70.99	-73.96	-2.07	0.9
2*f1-f3	63	-74.77	-81.25	-90.63	6.48	15.86
2*f1-f2	64	-75.02	-81.93	-91.19	6.91	16.17
f1+f2-f3 5*f2-4*f3	66	-70.37	-79.9	-86.8	9.53	16.43
f1	**67**	**-9.935**	**-9.954**	**-9.9**	**0.019**	**-0.035**
F1-f2+f3	68	-73.52	-86.93	-80.93	13.41	7.41
2*f2-f3 3*f2-2*f3	68.99	-79.08	-92.78	-85.1	13.7	6.02
f2	**70**	**-10.7**	**-10.66**	**-10.69**	**-0.04**	**-0.01**
f3	**71**	**-9.614**	**-9.596**	**-9.6**	**-0.018**	**-0.014**
2*f3-f2	72	-82.07	-90.11	-82.54	8.04	0.47
2*f2-f1 3*f3-2*f2	72.99	-77.8	-84.74	-88.67	6.94	10.87
f1+f2+f3 4*f3-3*f2	74	-69.17	-76.84	-82.5	7.67	13.33
2*f3-f1 5*f1-4*f3	75	-75.55	-82.8	-91.86	7.25	16.31
Spectral purity [dBc]		58.47	66.14	70.23	7.67	11.76

Table 5-2 Summary of the results using the general model, case II

Table 5-2 summarized the results for case II - group A. Those results show the greatest spectral purity obtained for the ninth polynomial degree pre-distorter, with 70.23 dBc. The reduction of the spurious level in the best case was similar to case I (around 16.5 dB) and achieved for ninth degree.

Case III

The power spectrum of the SG with a three tone signal at 67, 68, and 71 MHZ is shown in the following figures.

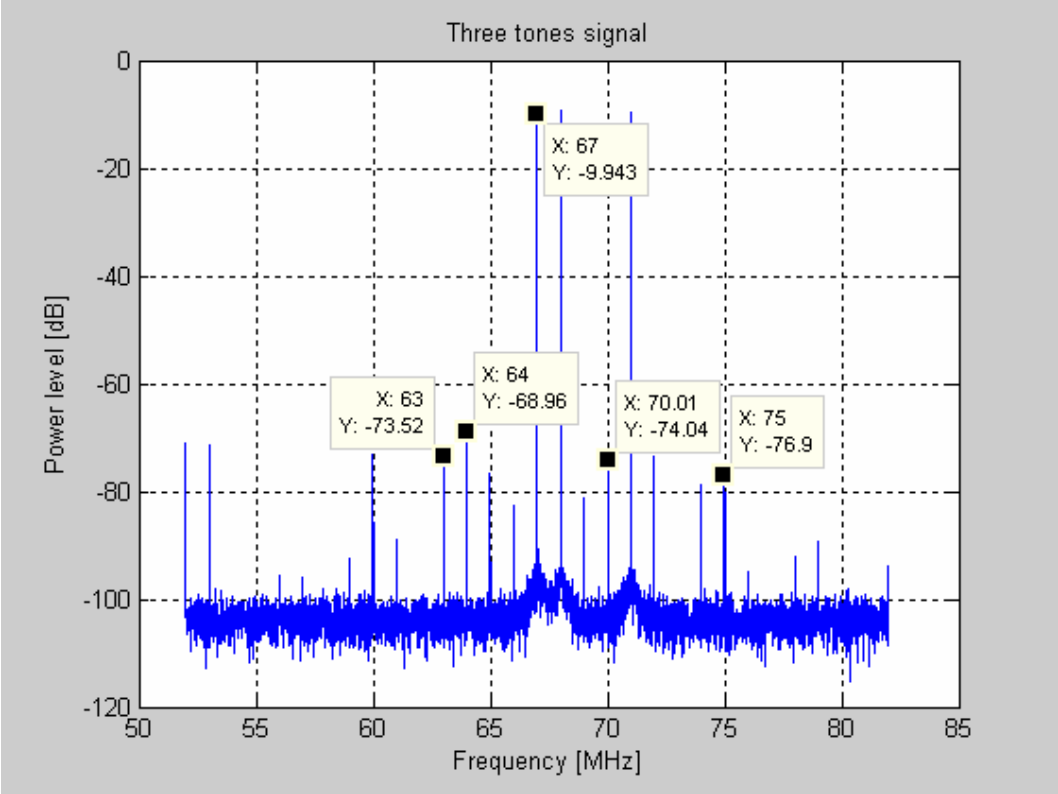

Figure 5.7 Power spectrum of the SG without pre-distortion, case III

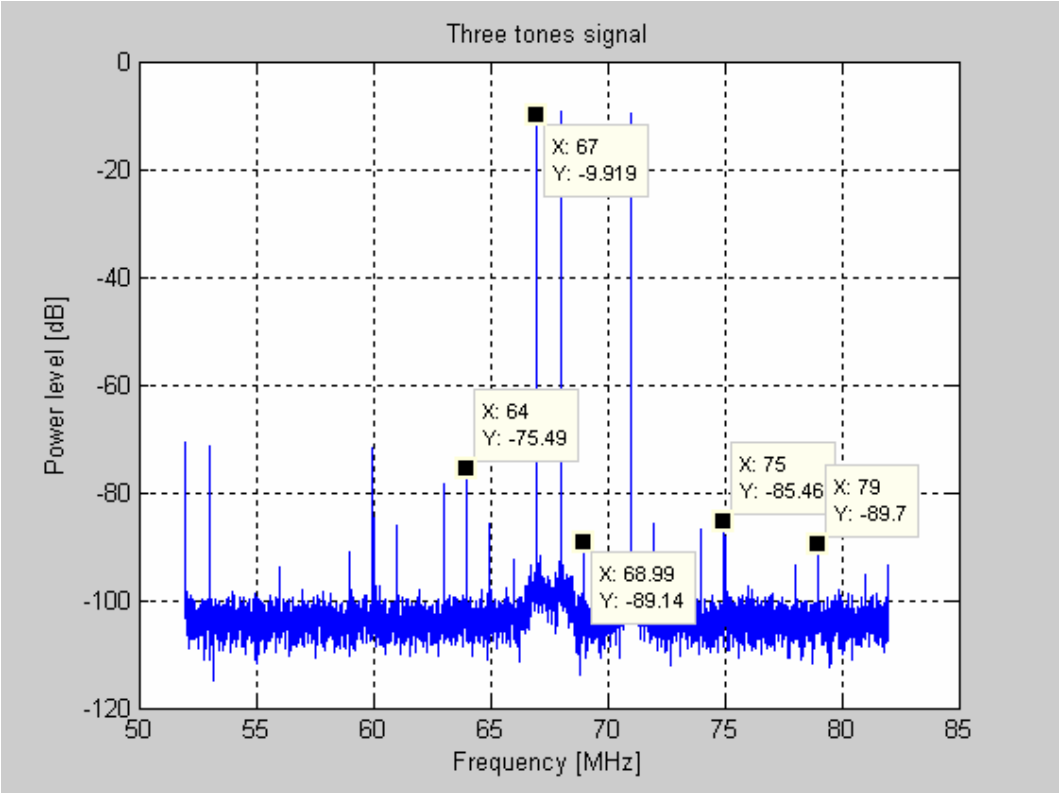

Figure 5.8: Power spectrum of the SG with PD of the fifth degree, case III

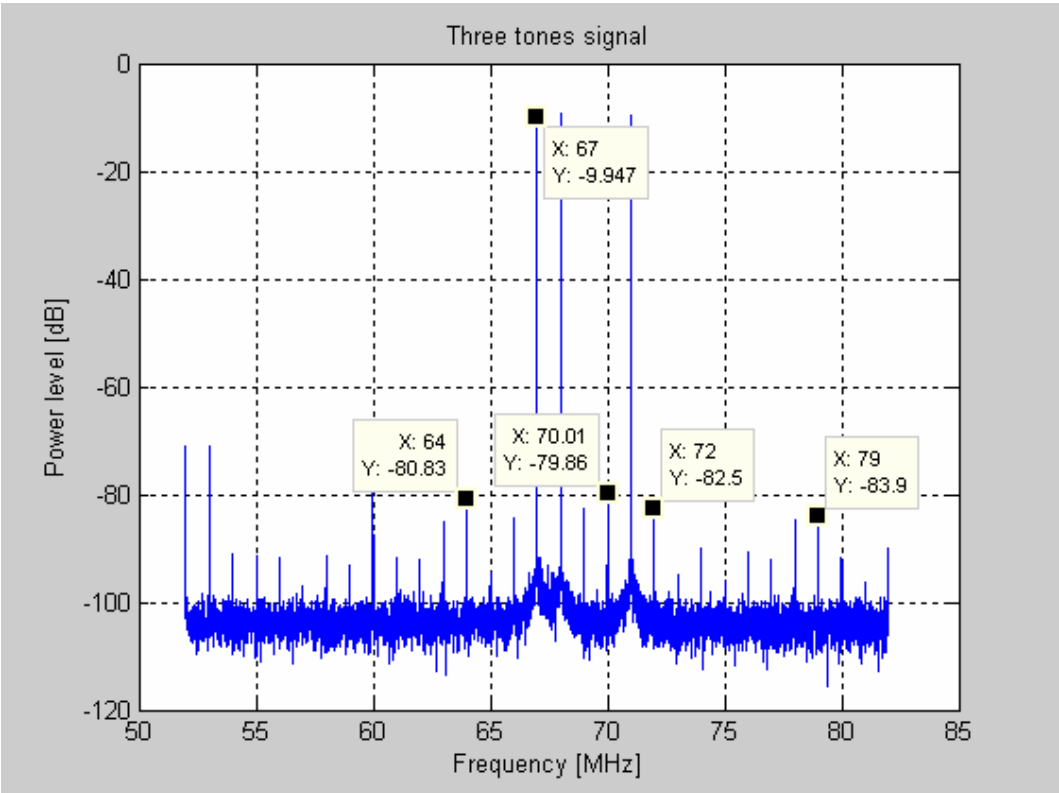

Figure 5.9: Power spectrum of the SG with PD of the ninth degree, case III

The results corresponding to case III are summarized in table 5-3. The information presented in this table is equivalent to the one shown in table 5-1:

IMD & Three tone frequencies	Frequency [MHz]	Power Level (PL), without predistortion [dBm]	PL with predistortion of fifth degree [dBm]	PL with predistortion of ninth degree [dBm]	IM5 Reduction Spurious levels [dB]	IM9 Reduction Spurious levels [dB]
-	53	-71.53	-71.22	-71.53	-0.31	0
fc	60	-73.22	-71.58	-73.74	-1.64	0.52
-	60.99	-88.99	-86.21	-91.84	-2.78	2.85
2*f1-f3	63	-73.52	-78.58	-84.98	5.06	11.46
f1+f2-f3 4*f1-3*f2	64	-68.96	-75.49	-80.83	6.53	11.87
2*f2-f3	65	-76.83	-85.88	-94.53	9.05	17.7
2*f1-f2	66	-82.58	-92.44	-84.33	9.86	1.75
f1	**67**	**-9.943**	**-9.9**	**-9.947**	**-0.043**	**0.004**
f2	**68**	**-9.358**	**-9.3**	**-9.3**	**-0.058**	**-0.058**
2*f2-f1	68.99	-81.35	-89.14	-82.57	7.79	1.22
f1-f2+f3 3*f2-2*f1	70	-74.04	-97.35	-79.86	23.31	5.82
f3	**71**	**-9.6**	**-9.6**	**-9.6**	**0**	**0**
-f1+f2+f3 4*f2-3*f3	72	-73.6	-85.94	-82.5	12.34	8.9
2*f3-f2	74	-78.72	-86.95	-90.12	8.23	11.4
2*f3-f1	75	-76.9	-85.46	-95	8.56	18.1
3*f3-2*f1	79	-89.34	-89.7	-83	0.36	-6.34
Spectral purity [dBc]		59.017	65.547	69.883	6.53	10.87

Table 5-3 Summary of the results using the general model, case III

The highest spectral purity observed was similar to the previous two cases, it was equal to 69.96dBc for the ninth polynomial degree. The major spurious reduction was of 18.1 dB for the ninth degree and 23.31 dB for the fifth degree. Both reductions were observed at IM3 frequency.

Group B

Group B evaluates the same cases mentioned above, only that the model coefficients that characterize the SG and build the pre-distorter are computed and applied in each case. Input power of -5 dBm and 0^{o} phase shift was used in the three cases.

Case I

Figures 5.4, 5.5, and 5.6 show the measurement results for case I.

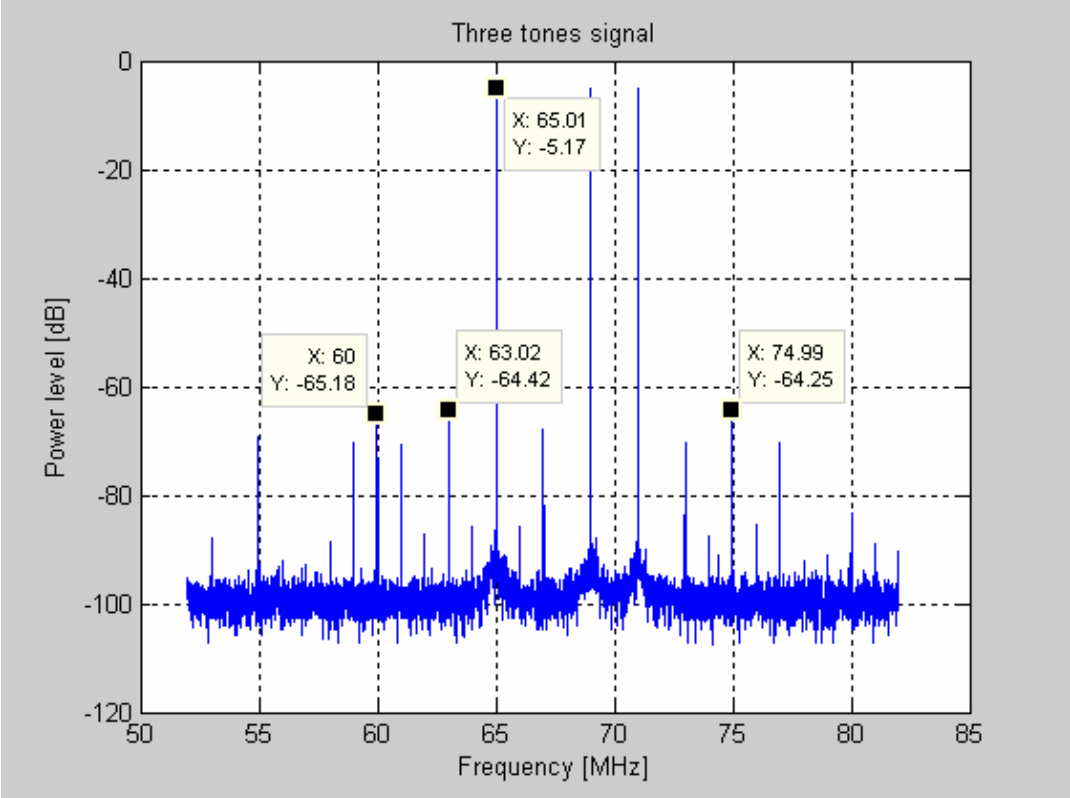

Figure 5.10 Power spectrum of SG without pre-distortion, case I

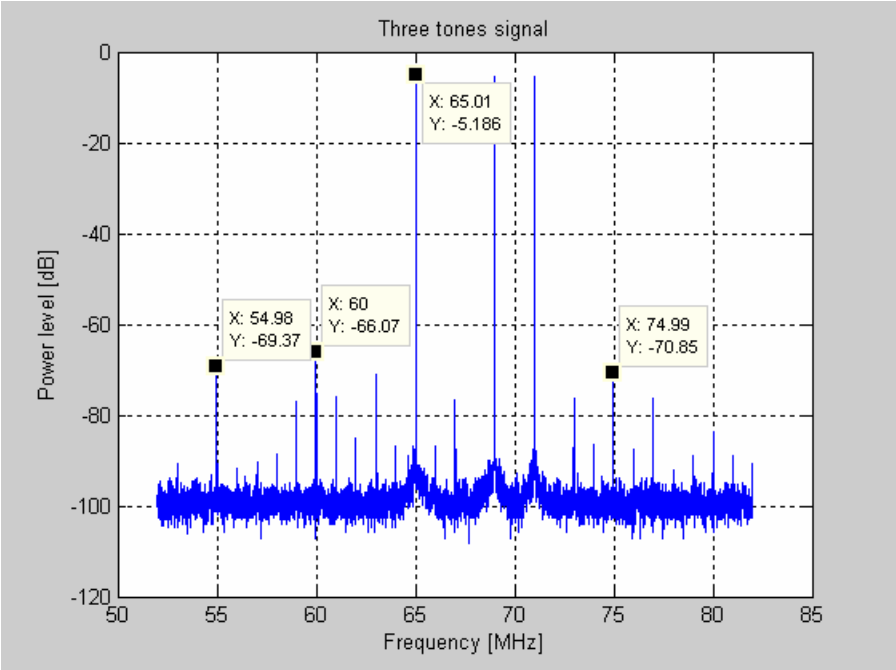

Figure 5.11 Power spectrum of SG with pre-distortion of fifth degree, case I

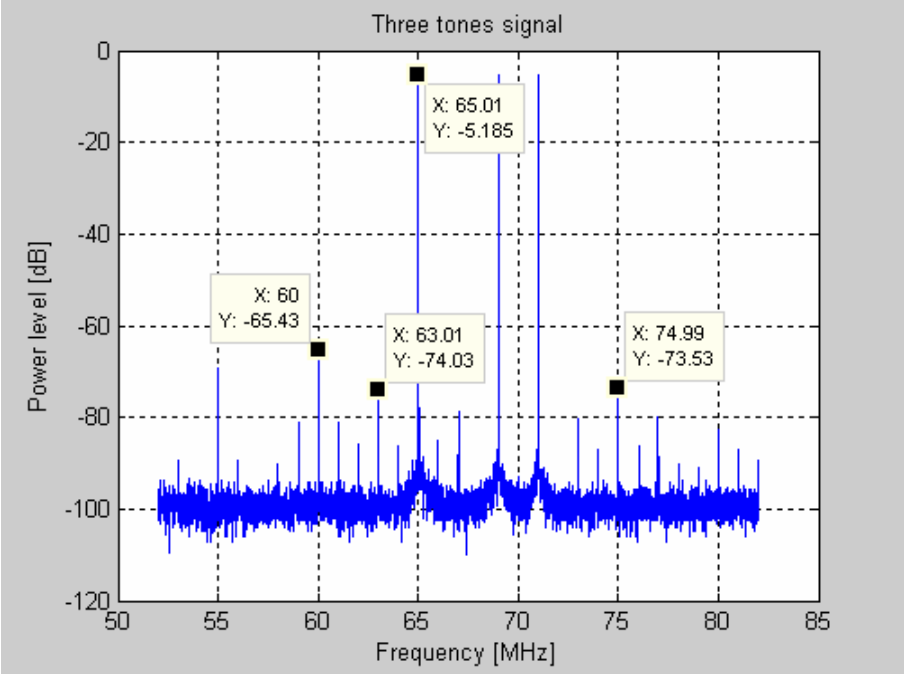

Figure 5.12 Power spectrum of SG with pre-distortion of ninth degree, case I

The obtained results for case I – group B are presented in table 5-4.

IMD & Three tone frequencies	Frequency [MHz]	Power Level (PL), without predistortion [dBm]	PL with predistortion of fifth degree [dBm]	PL with predistortion of ninth degree [dBm]	IM5 Reduction Spurious levels [dB]	IM9 Reduction Spurious levels [dB]
4*f1-3*f2	52.98	-88.05	-90.75	-89.35	2.7	1.3
4*f1-3*f3	54.98	-69.31	-69.38	-69.23	0.07	-0.08
f2-f1+f3	59.03	-70.46	-77	-82.83	6.54	12.37
fc	60	-65.18	-66.07	-65.43	0.89	0.25
2*f1-f2,5*f2-4*f3	61.02	-70.57	-76.05	-81.15	5.48	10.58
f1+f2-f3,4*f2-3*f3,4*f2-3f3*	63.01	-64.42	-71.1	-74.03	6.68	9.61
4*f1-3*f2,4*f1-3*f2	63.99	-85.74	-86.8	-86.36	1.06	0.62
f1	**65.01**	**-5.17**	**-5.186**	**-5.185**	**0.016**	**0.015**
3*f2-2*f3	65.99	-85.92	-86.8	-84.92	0.88	-1
f2	**69**	**-5.241**	**-6.106**	**-6.084**	**0.865**	**0.843**
f3	**71**	**-5.254**	**-5.277**	**-5.276**	**0.023**	**0.022**
2*f2-f1, 2*f3-f2	72.99	-70.51	-76.17	-80.34	5.66	9.83
3*f3-2*f2, -f1+f2+f3	74.99	-64.25	-70.85	-73.53	6.6	9.28
2*f3-f1,3*f2-2*f1,4*f3-3*f2	76.99	-70.4	-76.39	-79.77	5.99	9.37
Spectral Purity(dBc)		59.009	65.66	68.35	6.86	9.35

Table 5-4 Summarized results for group B, case I.

Looking at the above figures and table 5-4, one can notice the highest spurious' levels at frequencies belonging to the IM3 and in less quantity belonging to IM5 or IM7. The main reduction in the spurious' levels was observed at frequencies corresponding to the IM3 product equal to 12.37 dB.

Case II

Figures 5.13 to 5.15 exhibit the measurement results for case III – group B.

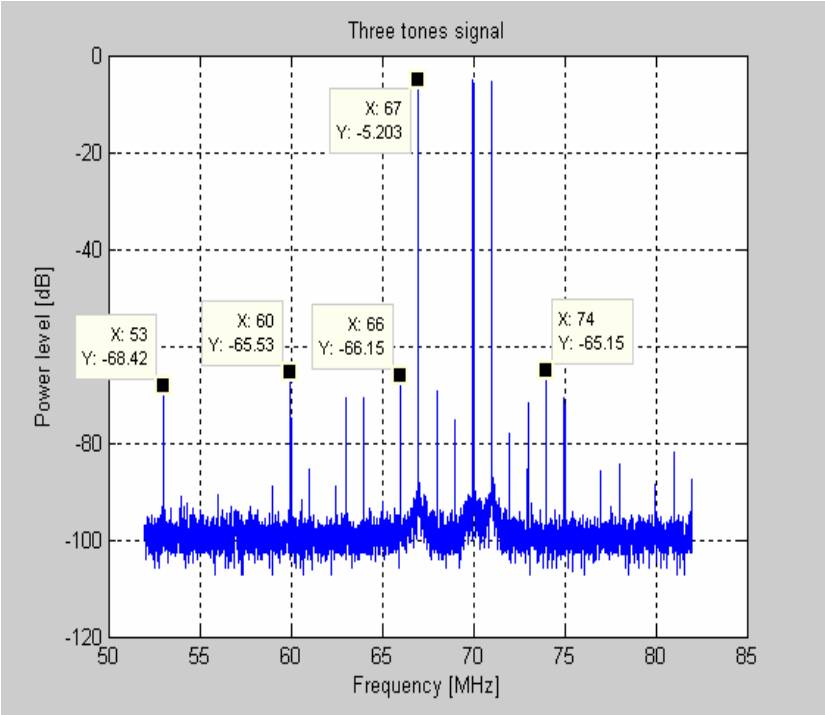

Figure 5.13 Power spectrum of SG without pre-distortion, case II

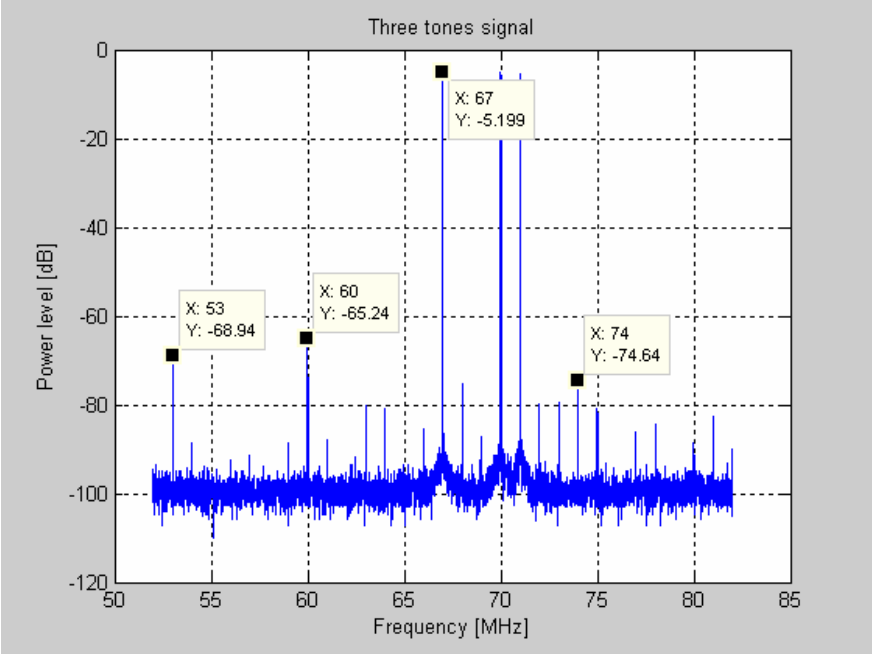

Figure 5.14 Power spectrum of SG with pre-distortion of fifth degree, case II

Table 5-5 resumes the information of measurements presented in Figures 5.13, 5.14, and 5.15

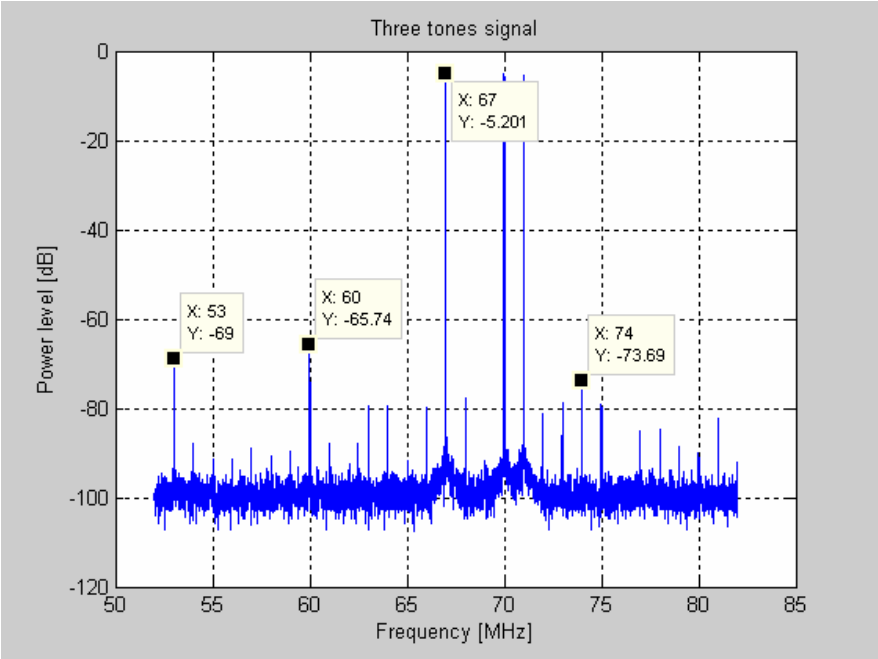

Figure 5.15 Power spectrum of SG with pre-distortion of ninth degree, case II

IMD & Three tone frequencies	Frequency [MHz]	Power Level (PL), without predistortion [dBm]	PL with predistortion of fifth degree [dBm]	PL with predistortion of ninth degree [dBm]	IM5 Reduction Spurious levels [dB]	IM9 Reduction Spurious levels [dB]
-	53	-68.42	-68.94	-69	0.52	0.58
fc	60	-65.53	-65.24	-65.74	-0.29	0.21
3*f1-2*f2	61	-85.49	-87.77	-88.05	2.28	2.56
2*f1-f3	63	-70.53	-80.33	-79.4	9.8	8.87
2*f1-f2	64	-70.66	-80.32	-79.4	9.66	8.74
5*f2-4*f3	66	-66.15	-85.39	-79.97	19.24	13.82
f1	**67**	**-5.203**	**-5.199**	**-5.201**	**-0.004**	**-0.002**
3*f2-2*f3	68	-69.17	-75.35	-77.76	6.18	8.59
2*f2-f3	68.99	-75.34	-87.29	-93.57	11.95	18.23
f2	**70**	**-5.874**	**-5.98**	**-5.88**	**0.106**	**0.006**
f3	**71**	**-5.267**	**-5.265**	**-5.264**	**-0.002**	**-0.003**
2*f3-f2	72	-78.14	-79.77	-81.12	1.63	2.98
2*f2-f1,3*f3-2*f2	72.99	-72.11	-79.91	-78.92	7.8	6.81
4*f3-3*f2,4*f3-3*f2	74	-65.15	-74.64	-73.69	9.49	8.54
2*f3-f1	75	-70.83	-80.76	-79.08	9.93	8.25
Spectral Purity [dBc]		59.95	69.44	68.49	9.49	8.54

Table 5-5 Summary of results for measurement case II

The results in table 5-5 show the lowest spurious levels after pre-distortion were equal to 9.49dB for the fifth degree, and a spectral purity of 69.44 dBc was obtained for the same order. The main reduction in the spurious levels was observed equal to 18.23 (ninth degree).

Case III

Figures 5.16, 5.17, and 5.18 show responses obtained when the three tone signal is at 67, 68, and 71 MHz frequencies.

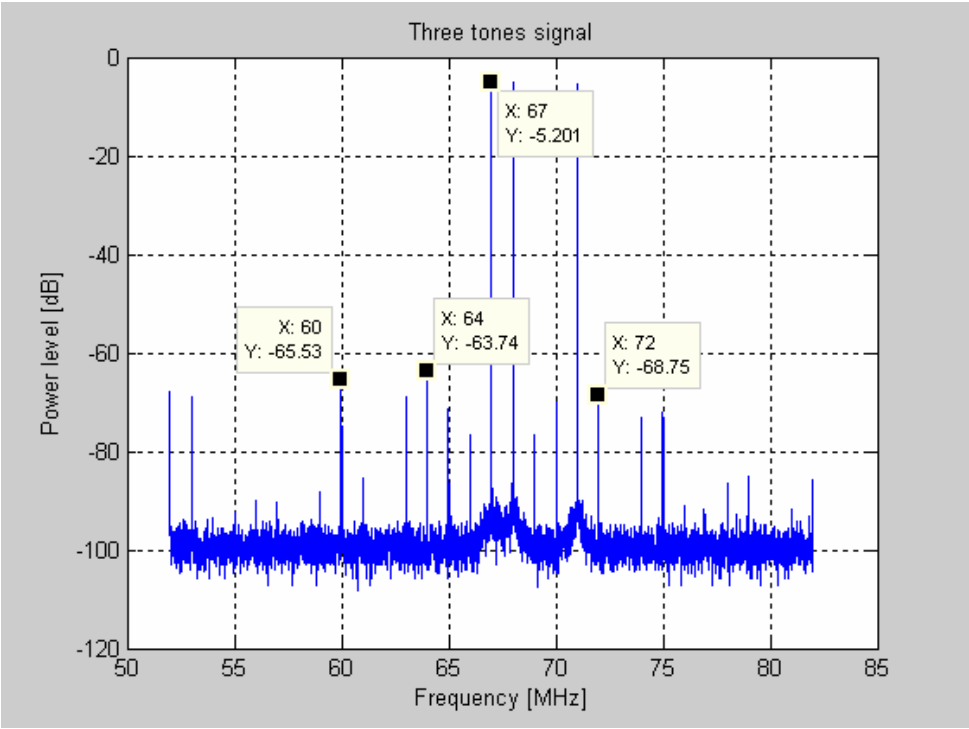

Figure 5.16 Power spectrum of SG without pre-distortion, case III

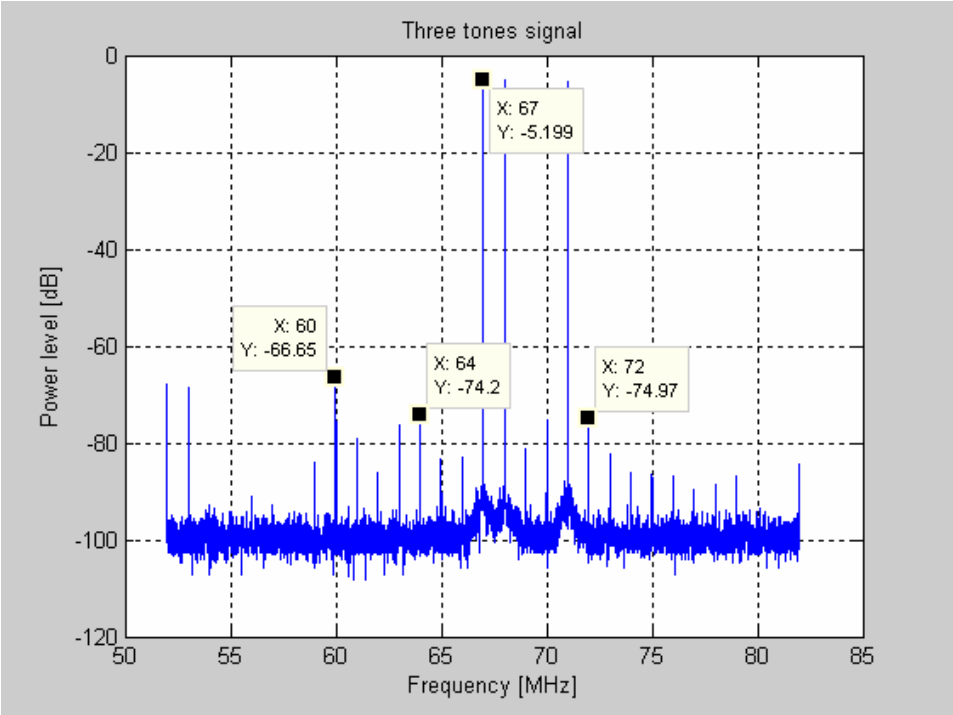

Figure 5.17 Power spectrum of SG with pre-distortion of fifth polynomial degree, case III

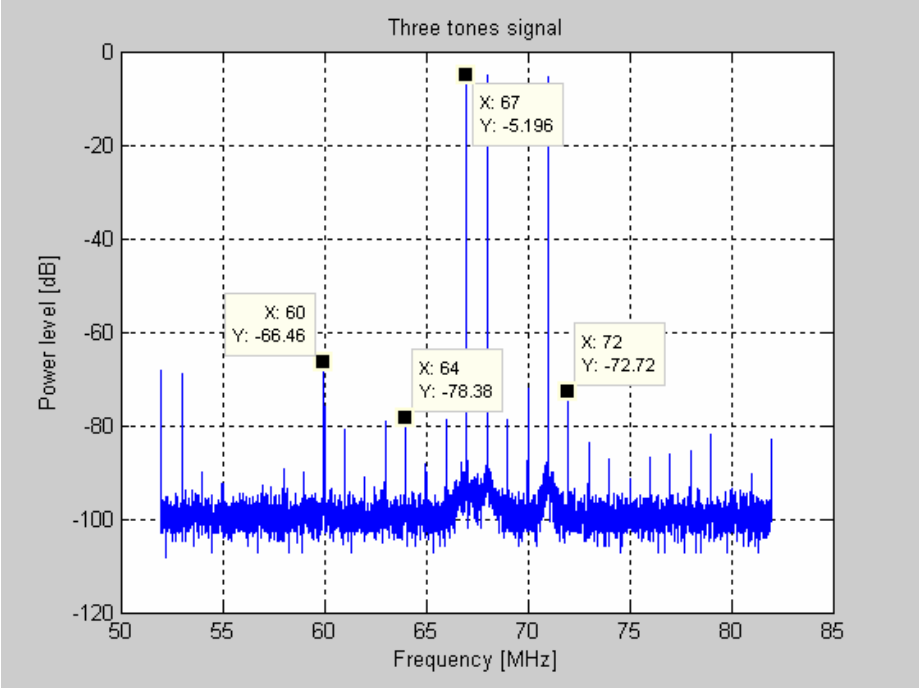

Figure 5.18 Power spectrum of SG with pre-distortion of ninth degree, case III

Table 5-6 gives a global idea about the improvements or impairments obtained from the measurements of case III – group B.

IMD frequencies & Three tone signal	Frequency [MHz]	Signla level (PL), without predistortion [dBm]	PL with predistortion of fifth degree [dBm]	PL with predistortion of ninth degree [dBm]	IM5 Reduction Sperious levels [dB]	IM9 Reduction Sperious levels [dB]
-	52	-67.82	-68	-68.4	0.18	0.58
-	53	-68.77	-68.54	-69	-0.23	0.23
5*f2-4*f3	56	-89.85	-91.14	-92	1.29	2.15
	56.99	-90.38	-94.8	-89.35	4.42	-1.03
4*f2-3*f3	59	-88.1	-84.21	-90.14	-3.89	2.04
fc	60	-65.53	-66.65	-66.49	1.12	0.96
f1+f2-f3	63	-69.1	-76.34	-79.12	7.24	10.02
f1+f2-f3,4*f1-3*f2,4*f1-3*f2	64	-63.74	-74.2	-78.38	10.46	14.64
2*f2-f3	64.99	-71.56	-83.33	-88.43	11.77	16.87
2*f1-f2,3*f2-2*f3	66.01	-76.58	-83.71	-79.84	7.13	3.26
f1	**67**	**-5.201**	**-5.199**	**-5.196**	**-0.002**	**-0.005**
f2	**68**	**-5.243**	**-5.24**	**-5.263**	**-0.003**	**0.02**
f1-f2+f3	70.01	-70.1	-75.17	-72.26	5.07	2.16
f3	**71**	**-5.566**	**-5.203**	**-5.203**	**-0.363**	**-0.363**
f2-f1+f3	71.99	-70.92	-74.97	-72.72	4.05	1.8
2*f3-f2	74.01	-73.04	-82.31	-87.04	9.27	14
2*f3-f1	75	-73.96	-86.03	-91	12.07	17.04
	78	-86.44	-88.62	-85	2.18	-1.44
Spectral Purity [dBc]		58.174	69.0	67	10.826	8.826

Table 5-6 Summarized results from the case III

In case III - group B the highest spectral purity achieved was equal to 69 dBc corresponding to the fifth polynomial degree. The greatest reduction in spurious level was 17.04 dB, for IM3. In contrast to the previous case, the results in case III- group B show better values for the fifth polynomial degree instead of ninth degree.

Group C

In group C the same cases were evaluated (I, II, and III), the same model of the SG was used to design the pre-distorter of ninth polynomial degree. However two different input powers were applied to analyze the differences in the reduction of spurious levels, number of unwanted frequencies generated due to the amplitude, and possible spectral purity for powers equal to : A=-5dBm and A=-10dBm.

Figures 5.19 and 5.20 exhibit the response obtained for input power equal -5 dBm.

Numerical values are presented in table 5-7.

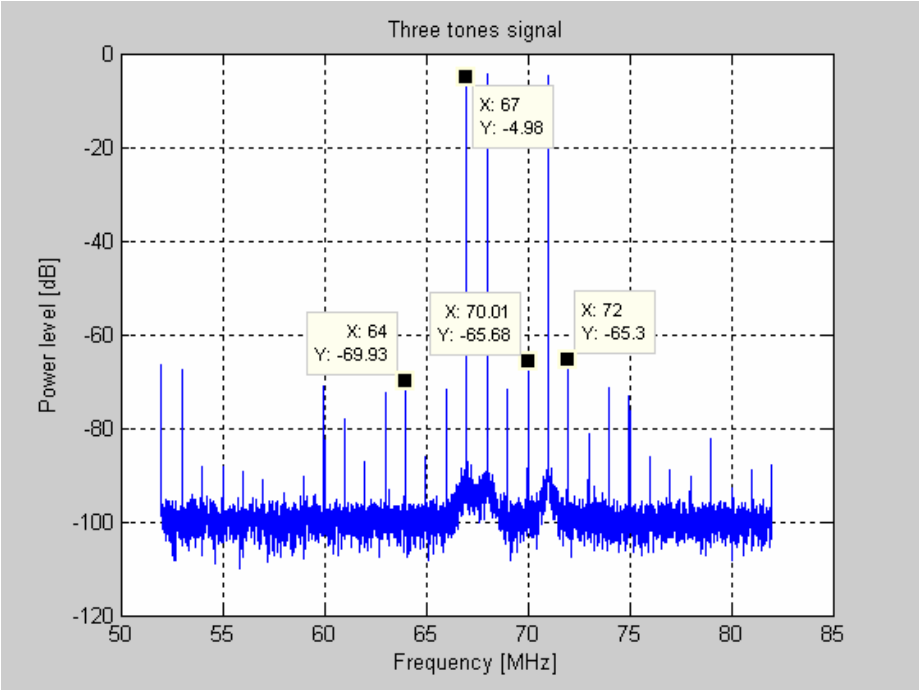

Figure 5.19 Power spectrum of SG with pre-distortion of ninth degree, case III, A=-5dBm

IMD frequencies & Three tone Frequency	Frequency [MHz]	Signal level (PL), without predistortion A = -5 dBm [dBm]	Signal level (PL), with predistortion ninth degree A = -5 dBm [dBm]	IM9 Reduction Spurious levels [dB]
-	53	-67.08	-67.58	0.5
fc	60	-68.9	-71.17	2.27
	60.99	-90	-78.24	-11.76
2*f1-f3	63	-60.67	-72.4	11.73
f1+f2-f3 4*f1-3*f2	64	-55.95	-69.93	13.98
2*f2-f3	65	-63.86	-86.04	22.18
2*f1-f2	66	-70.73	-71.71	0.98
f1	67	-5	-4.4	-0.6
f2	68	-4.3	-4.6	0.3
2*f2-f1	68.99	-66.01	-66.01	0
f1-f2+f3 3*f2-2*f1	70	-58.68	-65.68	7
f3	71	-4.6	-4.6	0
-f1+f2+f3 4*f2-3*f3	72	-58.68	-65.3	6.62
2*f3-f2	74	-63.69	-71.5	7.81
2*f3-f1	75	-62	-73.22	11.22
spectral purity [dBc]		51.65	60.7	9.05

Table 5-7: Summarized results from the measurement case III, A=-5dBm

From table 5-7 one can see the spectral purity achieved was 60.7 dBc. The improvement in the spectral purity was equal to 9.05 dB. However, the main reduction in spurious level was 22.18 dB for the IM3.

Figures 5.20 and 5.21, show the results when input power equals -10 dBm. Table 5-8 contains the values obtained from these measurements.

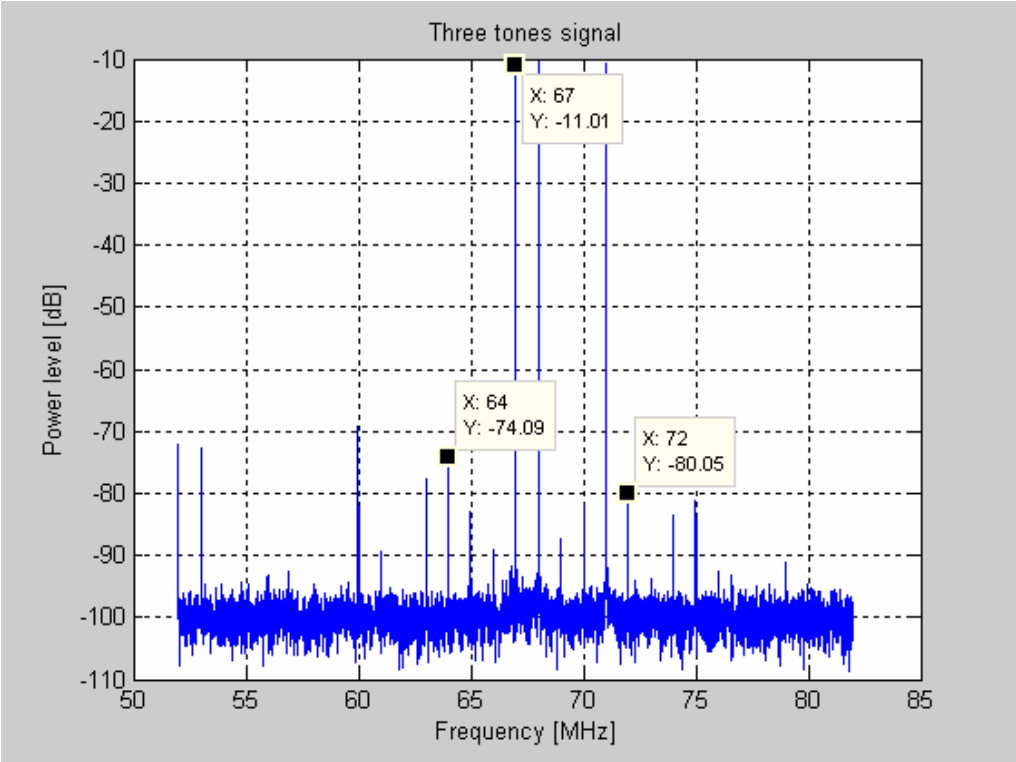

Figure 5.20 Power spectrum of SG without pre-distortion, case III, A=-10dBm

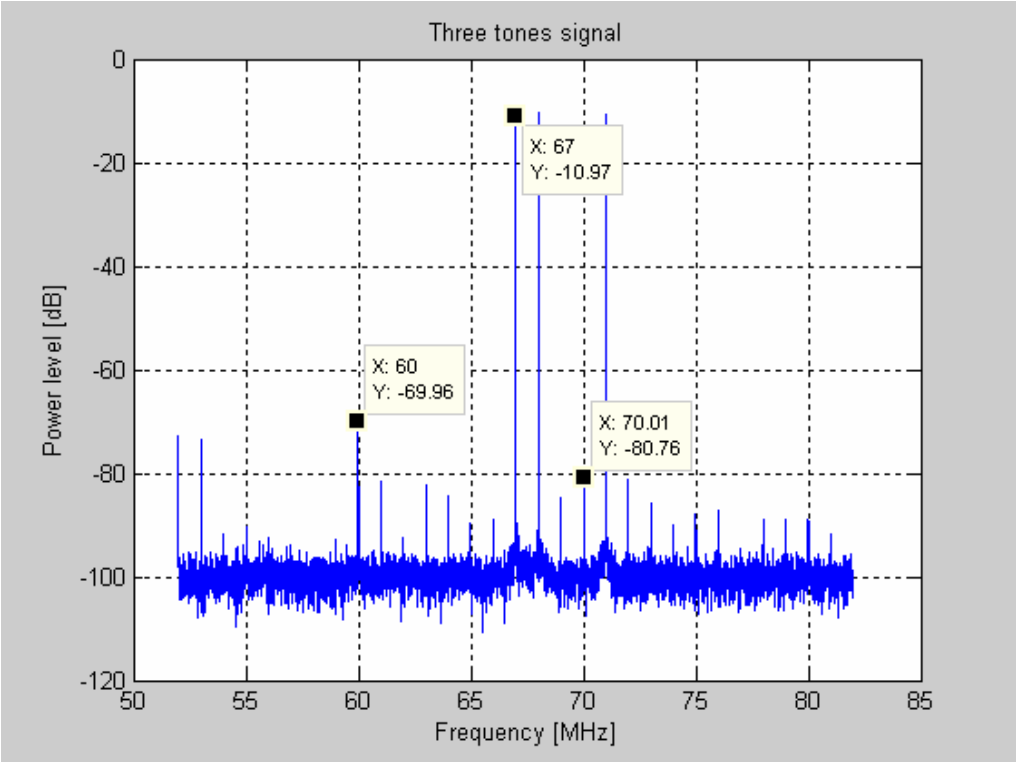

Figure 5.21 Power spectrum of SG with pre-distortion of ninth degree, case III, A=-10dBm

IMD frequencies & Three tone Frequency	Frequency [MHz]	Signal level (PL), without predistortion A = -10 dBm [dBm]	Signal level (PL), with predistortion ninth degree A = -10 dBm [dBm]	IM9 Reduction Spurious levels [dB]
-	53	-72.58	-73.59	1.01
-	60	-69.21	-69.96	0.75
-	60.99	-88.99	-82.23	-6.76
2*f1-f3	63	-77.65	-82.23	4.58
f1+f2-f3 4*f1-3*f2	64	-74.04	-84.22	10.18
2*f2-f3	65	-82.94	-89.67	6.73
2*f1-f2	66	-89.08	-92.44	3.36
f2	67	-11.01	-9.9	-1.11
f3	68	-10.01	-9.3	-0.71
2*f2-f1	68.99	-87.24	-84.84	-2.4
f1-f2+f3 3*f2-2*f1	70	-81.69	-80.76	-0.93
f3	71	-10.65	-10.65	0
-f1+f2+f3 4*f2-3*f3	72	-80.05	-81.13	1.08
2*f3-f2	74	-83.5	-90.11	6.61
2*f3-f1	75	-81.07	-87.27	6.2
spectral purity [dBc]		63.09	69.76	6.67

Table 5-8: summarized results for the measurement case III, A=-10dBm

Table 5-8 shows a spectral purity of -69.76dBc after the correction with the pre-distorter. The greatest reduction in spurious level this time was 10.18 dB again for IM3.

Summarizing, the spectral purity without pre-distortion obtained for input power of -10 dBm was better compared to the one observed for an input power of -5 dBm. However, spectral purity achieved (9.05 dB see table 5.7) is better with an input power of -5dBm.

6 Conclusions

The main goal in this thesis work was to develop a general method to generate spectrally pure signals using a model-based pre-distortion for signal generators.

The theory about model-based predistortion, nonlinear behavior, and intermodulation products was reviewed in order to explain and design the pre-distorter. Using pre-distortion; the nonlinearities and other imperfections in the generator will reduce the problems with harmonic distortion and intermodulation products in the generated signal. In order to design a pre-distorter, the signal generator characteristic was used to develop a model for the SG. The characteristic was obtained using polynomial system identification and Matlab.

The digital predistortion technique used in this work offers the simplicity and almost zero cost compared to analog predistortion. The polynomial degrees used for the predistortion were of fifth and ninth degree.

In order to see if the coefficients obtained represent the SG properly under different conditions, three groups were made: A, B, and C. Groups A and B were made to test if the model coefficients can be used for different frequencies. Group C is used to test if the model can be used for different amplitude levels and how much does the effectiveness of the pre-distorter vary. The confrontation of the results obtained in groups A and B shows that the proposed method can reproduce the SG in an accurate and robust way. On the other hand, group C showed that the spectral purity was better for the input power A = -10 dBm and equal to 69.76 dBc however the highest correction reach with the pre-distorter (ninth degree), was observe for the case of input power A = -5 dBm, this correction was equal to 9.05 dB against to 6.67 dB got it for the A = -10 dBm. The measurements confirmed the theoretical assumption that the main distortion is produced by IMD. However, the results also showed that this system shouldn’t be considered memoryless and therefore the applied pre-distortion method is only valid for a limited set of frequencies.

Summarizing, from the results of groups A and B the highest value of spectral purity obtained was approximately 70dBc in all cases. The ninth degree polynomial gave the best results in reduction of spurious levels with highest value of 18.23dBm in group A,

case III. In group C the best reduction of spurious' level was obtained for an input power of -5 dBm, in the case of a ninth degree polynomial.

The results confirmed that the model works fine for a limited set of frequencies and results in improvement compared to the situation when predistortion is not being used. The reason for which the model is frequency-dependent is that memory effects are present in the system and those effects were not taken into account in this model. It should be mentioned that the negative values of reduction in spurious values, are the consequence of new additional higher order distortion from the pre-distorter that were absent in the original SG spectrum.

Future work on this topic could be to use a model, such a Hammerstein, or Wiener [16], that considers memory effects. This will result in a more general and accurate model yielding better spectral purity, without limitation in frequency or dependency of the kind of generated signal. If one wished to further explore the memoryless method, it would be interesting to consider in the design of the pre-distorter the effects of the additional higher order terms introduced by the pre-distorter itself, and take a second measurement to add the parameters obtained to the first set of parameters.

References

[1] D. V. M. Rabijns, W.; Vandersteen, G., "Spectrally pure excitation signals: only a dream?," in *Instrumentation and Measurement, IEEE Transactions on*, vol. 53, 2004.

[2] M. Mansour, "Spectrally Pure Generation Based on Spectrum Analyser Measurements Using Pre-distortion," in *Department of technology*, vol. Master thesis. Gavle: University of Gavle, 2006.

[3] D. W. N. Björsell, N. Keskitalo, P. Händel, "Improved dynamic range for multi-tone signal using pre-distortion," 2006.

[4] D. Wisell, "A Baseband Time Domain Measurement System for Dynamic Characterisation of Power Amplifier with High Dynamic Range over Large Bandwith " in *Signals and Systems*. Uppsala: Uppala, 2004.

[5] H. K. a. J. S. Kenney, ""Behavioral Modeling of Nonlinear RF Power Amplifiers considering Memory effects "," *IEEE Transactions on Microwave Theory and Techniques*, vol. 52, 2003.

[6] R. H. Q. Z. Raich, G.T, "Orthogonal polynomials for power amplifier modeling and predistorter design," *IEEE Transactions on Microwave Theory and Techniques*, 2004.

[7] J. W. Zhang, Qiang Hao, Qing, "LUT Predistortion Based On Measured Non-Linear Characteristics of Power Amplifier," in *Department of Electronic Engineering*. China, 2007.

[8] S. P. McBeath, D., "Digital memory-based predistortion," *Microwave Symposium Diges*, 2005 IEEE MTT-S International.

[9] D. T. W. a. R. E. Kearney, *Identification of Nonlinear Physiological Systems*, 2003.

[10] M. I. N. Björsell, P. Händel, D.Rönnow, "Kautz-Volterra modelling of an analogue-to-digital converter using a stepped three-tone excitation," in *12th workshop on ADC Modeling and Testing* Iasi-Romania, 2007.

[11] P. S. N. Björsell, P. Händel, and D. Rönnow, "Measuring Volterra kernels of analog to digital converters using a stepped three-tone scan," in *IEEE trans. on Instrumentation and Mesurement*, 2006.

[12] Maxim, "Coherent Sampling Calculator," 2005.

[13] N. Ceylan, "Linearization of power amplifiers by means of digital predistortion," in *Technische Fakultät*, vol. Doctor-Ingenier. Erlangen: Universität Erlangen-Nürnberg, 2005.

[14] S. C. Cripps, *Advance Techniques in RF Power Amplifier Design* 2002.

[15] M. H. Hayes and 1996., *Statistical digital signal processing and modeling* New York

[16] M. Isaksson, "Behavioral Modellling of Radio Frequency," in *Engineering Sciences*, vol. Technical Licentiate in Signal Processing. Uppsala: Uppasala University, 2005.

[17] Agilent, "Vector Signal Analyzer Basic," 2004.